Brain Tumours

Mohammod Raziul Haque, Robert Ahmed Khan, S.I.M. Khairun Nabi Khan and Forhad H. Chowdhury

Abstract: Primary brain neoplasms can be benign or malignant. Primary neoplasms can originate from the brain parenchyma (intrinsic), meninges, cranial nerves, pituitary gland, choroid plexus, and from the ventricles. Primary malignant brain tumours have an annual global age-standardized incidence of 3.7/100,000 for men and 2.6/100,000 for women, with mortality rates of 2.8 per 100,000 for men and 2.0 per 100,000 for women. Common intracranial malignant tumours are glioma, ependymoma, medulloblastoma, and secondary metastatic tumours, whereas common benign tumours are meningioma, schwannoma, and sellar and suprasellar tumours. Clinical presentation depends on site, size, and on the age of the patient. The most common presentations include headache, seizure, features of raised ICP, and focal neuro-deficit/s. A CT scan and an MRI of the head with contrast are enough for diagnosing most brain tumours. Surgery is the primary modality of management. Surgical approaches differ according to size, site, age, nature of neoplasm, and operator experience and expertise as well. Prognosis depends on histological type, extent of resection, and postoperative therapy (where needed) as well. In this chapter, we will briefly discuss the surgical management of the most common brain tumours.

Abbreviations

ACTH	adrenocorticotrophin hormone	ADC	afferent diffusion co-efficient
AVM	arteriovenous malformation	BAER	brainstem auditory evoked response
BBB	blood–brain barrier	BCNU	biodegradable carmustine
CNS	central nervous system	CTV	clinical target volume
CT	computed tomography	CSF	cerebrospinal fluid
CUSA	Cavitron ultrasonic aspirator	DI	diabetes insipidus
DEBS	direct electrical brain stimulation	DTI	diffusion tensor imaging
DSA	digital subtraction angiogram	ECoG	Electrocorticogram
DW	diffusion-weighted	EEG	electroencephalogram
FIEST	fast imaging employing steady-state acquisition	ETV	endoscopic third ventriculostomy
EOR	extent of resection	FDG-PET	flurodeoxyglucose PET
EVD	external ventricular drainage	FSH	follicle-stimulating hormone
fMRI	functional magnetic resonance imaging	GTV	gross tumour volume
GTR	gross total resection	HGG	high-grade glioma
HCG	human chorionic gonadotrophin	ICG	indocyanine green
HPC	Hemangiopericytoma	iMRI	intraoperative MRI
ICP	intracranial pressure	IPS	inferior petrosal sinus
IDH	isocitrate dehydrogenase	KPS	Karnofsky performance status
IMRT	intensity-modulated radiotherapy	LH	luteinizing hormone
LGG	low-grade glioma	MB	Medulloblastoma
LINAC	linear accelerator	MEG	magneto encephalography
MRI	magnetic resonance imaging	MEP	motor evoked potential
MRA	magnetic resonance angiogram	NAA	N-acetyl aspartate
MRS	magnetic resonance spectroscopy	OS	overall survival
PET	positron emission tomography	PFS	progression-free survival
PTV	planning target volume	SPECT	single-photon emission computed tomography
SEP	sensory evoked potential	SFT	solitary fibrous tumour
SSS	superior sagittal sinus	SRS	stereotactic radiotherapy
TCD	transcranial doppler	TMZ	Temozolomide
TSH	thyroid-stimulating hormone	USG	Ultrasonogram
VEP	visual evoked potential	VDE	velocity of diametric expression
VPS	ventriculoperitoneal shunt	WBRT	whole-brain radiotherapy
XRT	X-ray radiotherapy		

1. Incidence/Epidemiology

Primary malignant brain tumours have an annual global age-standardized incidence of 3.7/100,000 for men and 2.6/100,000 for women, with mortality rates of 2.8 and 2.0 per 100,000 for men and for women (GLOBOCAN 2002). In the USA, the incidence of both non-malignant and primary malignant brain tumours is 14.8/100,000 per year, with 6–8/100,000 having a high-grade neoplasm. The annual incidence rate of metastatic brain tumours is estimated to be 8.3–11/100,000 people. Tumour types are distributed differently by age. According to the Swedish Cancer Registry, the commonest types of tumours in paediatric cases aged 15 years and younger are medulloblastoma (23.5%) and low-grade glioma (31.7%); this is in stark contrast to adult cases, where high-grade glioma (30.5%) and meningioma (29.4%) are the commonest types of adult primary brain neoplasms. The 5- and 10-year survival rates are 29.1% and 25.3%, respectively, according to the American Cancer Society (ACS; www.cancer.org), and vary greatly by age and histology. Glioblastoma multiforme (GBM) has a 5-year survival rate of 3.3%, while lower-grade gliomas like oligodendroglioma, pilocytic astrocytoma, and ependymoma have 5-year survival rates of over 70%. Astrocytoma (not otherwise specified), malignant glioma, anaplastic astrocytoma, and lymphoma have comparable overall survival rates. For the majority of histologies, five-year survival rates drop as people get older (www.cbtrus.org). However, some histologic categories (e.g., ependymoma and GBM) have a lower survival rate in paediatric patients and in the elderly. The disparity in incidence rates between men and women is one of the most constant findings in the epidemiology of brain tumours; glioma is more prevalent in men, while meningioma is more common in women (Newton 2016; Bondy et al. 2008).

In both population registry data and clinical trials, histologic grade and type, age, extent of resection, tumour site, radiation therapy, and various chemotherapy regimens have been consistently and conclusively associated with survival. GBM and anaplastic astrocytoma patients' survival is also predicted by their Karnofsky performance status (KPS) at diagnosis, as well as other measures of physical and mental capability (Levin et al. 2001).

2. Classification

In the 2016 update, molecular markers were incorporated into the histological classification of brain tumours for the first time. The main changes were in the glioma and medulloblastoma groups. In the context of glioma, "genotype trumps over phenotype", and classification is based on the assessment of IDH mutations as well as 1p/19q status in diffuse glioma (van den Bent et al. 2017). Diffuse midline glioma, H3 K27M-mutant, RELA fusion-positive ependymoma, embryonal tumour with multi-layered rosettes, C19MC-altered, and hybrid nerve sheath tumours are among the new additions. Protoplasmic and fibrillary astrocytoma, glioblastoma cerebri, and cellular ependymoma are among the variants and patterns that have been removed because they no longer have biological or diagnostic significance. Other changes include the removal of the term "primitive neuroectodermal tumour", the addition of a criterion for brain invasion in atypical meningioma, the distinction of melanotic schwannoma from other types of schwannoma, and the grouping of solitary fibrous tumours and haemangiopericytoma as a single entity. There is also an increase in the number of entities in nerve sheath tumours and CNS haematopoietic/lymphoid cancers (Gupta and Dwivedi 2017).

The sixth iteration of the global standard for the categorization of brain and spinal cord malignancies is the WHO Classification of Malignancies of the Central Nervous System (CNS), which was released in 2021. This is the fifth edition of this classification, updated in 2021 (Table 1), and it adds significant modifications that enhance the use of molecular diagnostics in CNS tumour classification, building on the work of the Consortium to Inform Molecular and Practical Approaches to CNS Tumor Taxonomy and on the fourth edition, published in 2016. However, it continues to be allied with other well-established methods of tumour diagnosis, like immunohistochemistry and histology. In doing so, the fifth edition highlights the significance of integrated diagnostics and layered reports while establishing some distinct approaches to CNS tumour nomenclature and grading. There is an introduction of new tumour kinds and subtypes, some of which are based on cutting-edge diagnostic tools like DNA methylome analysis. The main changes to tumour taxonomy introduced in the 2021 edition are outlined in this section, along with particular modifications to each taxonomic group (Louis et al. 2021).

Table 1. WHO classification of CNS tumours of 2021 is shown below.

1. Gliomas, Glioneuronal Tumours, and Neuronal Tumours
1.1 Adult-type diffuse gliomas
1.1.1 Astrocytoma, IDH-mutant
1.1.2 Oligodendroglioma, IDH-mutant, and 1p/19q-codeleted
1.1.3 Glioblastoma, IDH-wildtype
1.2 Paediatric-type diffuse low-grade gliomas
1.2.1 Diffuse astrocytoma, MYB- or MYBL1-altered
1.2.2 Angiocentric glioma
1.2.3 Polymorphous low-grade neuroepithelial tumour of the young (PLNTY)
1.2.4 Diffuse low-grade glioma, MAPK pathway-altered
1.3 Paediatric-type diffuse high-grade gliomas
1.3.1 Diffuse midline glioma, H3 K27-altered
1.3.2 Diffuse hemispheric glioma, H3 G34-mutant
1.3.3 Diffuse paediatric-type high-grade glioma, H3-wildtype and IDH-wildtype
1.3.4 Infant-type hemispheric glioma
1.4 Circumscribed astrocytic gliomas
1.4.1 Pilocytic astrocytoma
1.4.2 High-grade astrocytoma with piloid features
1.4.3 Pleomorphic xanthoastrocytoma
1.4.4 Subependymal giant-cell astrocytoma
1.4.5 Chordoid glioma
1.4.6 Astroblastoma, MN1-altered
1.5 Glioneuronal and neuronal tumours
1.5.1 Ganglioglioma
1.5.2 Desmoplastic infantile ganglioglioma/desmoplastic infantile astrocytoma
1.5.3 Dysembryoplastic neuroepithelial tumour
1.5.4 Diffuse glioneuronal tumour with oligodendroglioma-like features and nuclear clusters
1.5.5 Papillary glioneuronal tumour
1.5.6 Rosette-forming glioneuronal tumour
1.5.7 Myxoid glioneuronal tumour
1.5.8 Diffuse leptomeningeal glioneuronal tumour
1.5.9 Gangliocytoma
1.5.10 Multinodular and vacuolating neuronal tumour
1.5.11 Dysplastic cerebellar gangliocytoma (Lhermitte–Duclos disease)
1.5.12 Central neurocytoma
1.5.13 Extraventricular neurocytoma
1.5.14 Cerebellar liponeurocytoma
1.6 Ependymal tumours
1.6.1 Supratentorial ependymoma
1.6.1.1 Supratentorial ependymoma, ZFTA fusion-positive
1.6.1.2 Supratentorial ependymoma, YAP1 fusion-positive
1.6.2 Posterior fossa ependymoma
1.6.2.1 Posterior fossa ependymoma, group PFA
1.6.2.2 Posterior fossa ependymoma, group PFB
1.6.3 Spinal ependymoma
1.6.3.1 Spinal ependymoma, MYCN-amplified
1.6.4 Myxopapillary ependymoma
1.6.5 Subependymoma
2. Choroid Plexus Tumours
2.1 Choroid plexus papilloma
2.2 Atypical choroid plexus papilloma
2.3 Choroid plexus carcinoma
3. Embryonal Tumours
3.1 Medulloblastoma
3.2 Atypical teratoid/rhabdoid tumour
3.3 Cribiform neuroepithelial tumour
3.4 Embryonal tumour with multilayered rosettes
3.5 CNS neuroblastoma, FOXR2-activated
3.6 CNS tumour with BCOR internal tandem duplication

Table 1. *Cont.*

4. Pineal Tumours
4.1 Pineocytoma
4.2 Pineal parenchymal tumour of intermediate differentiation
4.3 Pineoblastoma
4.4 Papillary tumour of the pineal region
4.5 Desmoplastic myxoid tumour of the pineal region, SMARCB1-mutant
5. Cranial and Paraspinal Nerve Tumours
5.1 Schwannoma
5.2 Neurofibroma
5.3 Perineurioma
5.4 Hybrid nerve sheath tumour
5.5 Malignant melanotic nerve sheath tumour
5.6 Malignant peripheral nerve sheath tumour
5.7 Paraganglioma
6. Meningioma
Subtypes:
6.1 Meningothelial meningioma
6.2 Fibrous meningioma
6.3 Transitional meningioma
6.4 Psammomatous meningioma
6.5 Angiomatous meningioma
6.6 Microcystic meningioma
6.7 Secretory meningioma
6.8 Lymphoplasmacyte-rich meningioma
6.9 Metaplastic meningioma
6.10 Chordoid meningioma
6.11 Clear-cell meningioma
6.12 Atypical meningioma
6.13 Papillary meningioma
6.14 Rhabdoid meningioma
6.15 Anaplastic (malignant) meningioma
7. Mesenchymal, Non-Meningothelial Tumours
7.1 Soft-tissue tumours
7.1.1 Fibroblastic and myofibroblastic tumours
7.1.1.1 Solitary fibrous tumour
7.1.2 Vascular tumours
7.1.2.1 Haemangiomas and vascular malformations
7.1.2.2 Haemangioblastoma
7.1.3 Skeletal muscle tumours
7.1.3.1 Rhabdomyosarcoma
7.1.4 Uncertain differentiation
7.1.4.1 Intracranial mesenchymal tumour, FET-CREB fusion-positive
7.1.4.2 CIC-rearranged sarcoma
7.1.4.3 Primary intracranial sarcoma, DICER1-mutant
7.1.4.4 Ewing sarcoma
7.2 Chondro-osseous tumours
7.2.1 Chondrogenic tumours
7.2.1.1 Mesenchymal chondrosarcoma
7.2.1.2 Chondrosarcoma
7.2.2 Notochordal tumours
7.2.2.1 Chordoma (including poorly differentiated chordoma)
8. Melanocytic Tumours
8.1 Diffuse meningeal melanocytic neoplasms
8.1.1 Meningeal melanocytosis and meningeal melanomatosis
8.2 Circumscribed meningeal melanocytic neoplasms
8.2.1 Meningeal melanocytoma and meningeal melanoma

Table 1. *Cont.*

9. Haematolymphoid Tumours
9.1 Lymphomas
9.1.1 CNS lymphomas
9.1.1.1 Primary diffuse large B-cell lymphoma of the CNS
9.1.1.2 Immunodeficiency-associated CNS lymphoma
9.1.1.3 Lymphomatoid granulomatosis
9.1.1.4 Intravascular large B-cell lymphoma
9.1.2 Miscellaneous rare lymphomas in the CNS
9.1.2.1 MALT lymphoma of the dura
9.1.2.2 Other low-grade B-cell lymphomas of the CNS
9.1.2.3 Anaplastic large cell lymphoma (ALK+/ALK−)
9.1.2.4 T-cell lymphomas and NK/T-cell lymphomas
9.2 Histiocytic tumours
9.2.1 Erdheim–Chester disease
9.2.2 Rosai–Dorfman disease
9.2.3 Juvenile xanthogranuloma
9.2.4 Langerhans cell histiocytosis
9.2.5 Histiocytic sarcoma
10. Germ Cell Tumours
10.1 Mature teratoma
10.2 Immature teratoma
10.3 Teratoma with somatic-type malignancy
10.4 Germinoma
10.5 Embryonal carcinoma
10.6 Yolk sac tumour
10.7 Choriocarcinoma
10.8 Mixed germ cell tumour
11. Tumours of the Sellar Region
11.1 Adamantinomatous craniopharyngioma
11.2 Papillary craniopharyngioma
11.3 Pituicytoma, granular cell tumour of the sellar region, and spindle cell oncocytoma
11.4 Pituitary adenoma/PitNET
11.5 Pituitary blastoma
12. Metastases to the CNS
12.1 Metastases to the brain and spinal cord parenchyma
12.2 Metastases to the meninges

Source: Authors' compilation based on data from WHO Classification of Tumours Editorial Board (2021).

3. Intrinsic Brain Tumours

3.1. Gliomas

3.1.1. Introduction

Glioma susceptibility seems to be hereditary, according to studies of syndromes, linkage, familial aggregation, and mutagen sensitivity in adulthood. Syndromes including medulloblastoma or gliomas, with gene names and chromosome location, are neurofibromatosis 1 (NF1, 17q11) and 2 (NF2 22q12), retinoblastoma (RB1; 13q14), tuberous sclerosis (TSC1 9q34, TSC2 16p13), and Li–Fraumeni (TP53 17p13), as well as Turcot's syndrome and multiple hamartoma (APC 5q21, hMLH1 3p21.3, hMSH2 2p22-21, PMS2 7p22, PTEN 10q23.3) (Bondy et al. 2008). Gliomas are linked to a number of polymorphisms, the most prevalent of which are found in carcinogen metabolism, DNA repair, and immune function genes. Ionizing radiation in certain forms and doses is widely recognized as a cause of brain cancers (Ron 2003). There is yet to be a study that identifies a link between mobile phone use and the risk of having a brain tumour (Newton 2016). Meta-analyses of a large body of research based on multiple case–control and two cohort studies show that self-reported allergies are associated with glioma in a way that is unlikely to be due to chance or methodologic biases alone (Linos et al. 2007).

The WHO Revised 4th edition (2016) classification groups diffusely infiltrating gliomas (oligodendroglial tumours and astrocytic tumours) together and then introduces the category "Other astrocytic tumours" for astrocytomas that are more circumscribed (pleomorphic xanthoastrocytoma, pilocytic astrocytoma, subependymal

giant-cell astrocytoma). As a result, the term "low-grade glioma" (LGG) is used to refer to grade 2 gliomas as mentioned by the WHO, including diffuse astrocytomas, oligodendrogliomas, and oligoastrocytomas (Louis et al. 2016).

Supporting glial cells in the brain give rise to high-grade gliomas. The pathological classification is determined by the major cell type. According to the WHO grading system, tumours are rated based on light microscopy appearances (grade 1 to 4). WHO grade 3 (anaplastic astrocytoma and anaplastic oligoastrocytoma) and 4 tumours are classified as HGGs (glioblastoma with oligodendrocyte component, glioblastoma, gliosarcoma). Grade 4 tumours are diffusely infiltrating gliomas with focal or distributed anaplasia and a high proliferative capacity, as evidenced by distinct nuclear atypia, enhanced cellularity, and significant mitotic activity on histological examination. Cellular polymorphism, rapid mitotic activity, nuclear atypia, arterial thrombosis, necrosis, and microvascular proliferation are all seen in grade 4 tumours (Price et al. 2019). The introduction of the WHO Classification of Tumours of the CNS has resulted in broad changes in the categorization of high-grade glioma (Pallud et al. 2014). The definition of molecular subgroups has grossly divided glial-origin tumours into three categories: isocitrate dehydrogenase (IDH) wildtype, IDH mutated, and IDH not specified (i.e., where IDH mutation has not been sought). Within this classification (and with the inclusion of the 1p 19q chromosomal codeletion for oligodendroglioma), diffuse glioma, oligodendroglioma, anaplastic astrocytoma, anaplastic oligodendroglioma, and glioblastoma have now all been defined.

3.1.2. Clinical Considerations

LGGs present with seizures in more than 80% cases. Others present with focal neuro-deficits, altered mentation, or raised intracranial pressure (Pallud et al. 2014). Although "gross neurological deficits" such as dysphasia and hemiparesis are uncommon when LGGs appear, objective neuropsychological examinations generally reveal more subtle cognitive problems at the time of diagnosis. Executive function, attention, focus, working memory, and mood disorders are all common. Before beginning oncological treatment, a thorough evaluation of higher mental functions and health-linked quality of life is now suggested (Klein et al. 2012).

In patients with glioblastoma, the symptoms and indications are relatively uniform but nonspecific. Increased intracranial pressure, which can cause headache, vomiting and nausea, double or blurred vision, and drowsiness, is prevalent in affected people. Extraocular palsies, objective papilloedema, pupil irregularities, and a lower degree of consciousness may be related to these signs and symptoms. They are usually more noticeable in the morning and improve over the day. These tumours are characterized by unrelenting, increasing headache. Seizures affect up to a third of glioblastoma patients (Rincon-Torroella et al. 2017). Bases on the extent and location of tumour invasion, neurological deficits are prevalent. These deficits include changes in personality and altered cognition and might be localized or widespread (Tucha et al. 2000). Although neurological abnormalities from anaplastic astrocytoma and glioblastoma are widespread, they are often subtle and may go unnoticed until the brain tumour is discovered.

3.1.3. Neuroradiological Characteristics

Magnetic resonance imaging (MRI) of LGGs demonstrates tumours that are isointense/hypointense on T1W images, are homogeneously hyperintense on T2W images, and are not enhanced with contrast administration. The extent of the tumour has been shown to best correspond to FLAIR hyperintensity (Figure 1). However, it is important to remember that LGG is a diffuse neoplastic disease and that glioma cells have been shown to be present as far as 2 cm beyond FLAIR signal abnormality (Pallud et al. 2010). Sophisticated MRI techniques, such as MR spectroscopy, have been used to differentiate glioma grades and even to detect key LGG metabolic mutations, such as those of the isocitrate dehydrogenase 1 (IDH1) gene. When tumours were graded with use of proton MR spectroscopy of metabolite ratios (choline/N-acetylaspartate, choline/creatine, and N-acetylaspartate/creatine), this yielded significant differences between LGGs and HGGs ($P < 0.01$). An increased choline-creatinine ratio on MR spectroscopy corresponded to a heightened risk of transformation (Law et al. 2003). MRS of glioma generally shows a choline peak that is significantly increased, a decreased NAA peak, and a creatinine peak with no obvious change. With an increase in glioma malignancy degree, the choline peak increases even more. In some cases, an abnormal increase in the lactate peak or lipid peak could also be detected.

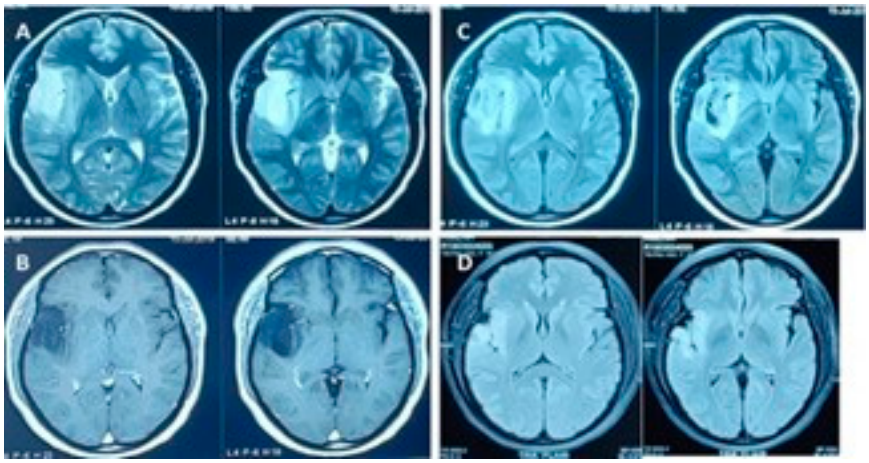

Figure 1. Low-grade gliomas are hyperintense on MRI T2W sequence (**A**), hypointense without contrast enhancement on T1W (**B**), and again hyperintense on FLAIR sequence (**C**). FLAIR sequence is the ideal follow-up sequence and, in this case, shows no tumour recurrence after 1 year (**D**). Source: Figure by authors.

For brain tumours, MRI is now the preferred method of investigation. On T1-weighted MRI, high-grade glioma generally presents as an irregular hypodense lesion with varying degrees of contrast enhancement and oedema (Figure 2).

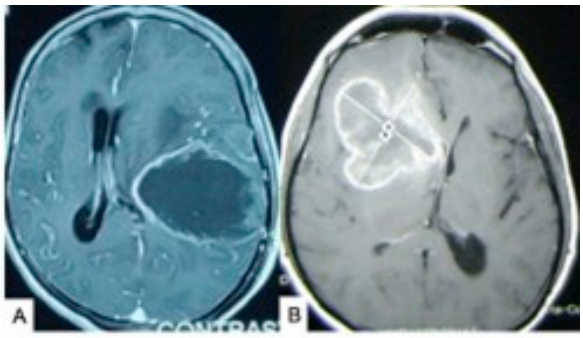

Figure 2. Glioblastomas are typically irregular, peripherally enhancing tumours with central necrosis and mass effect. Contrast MRI axial view: (**A**) parietal GBM and (**B**) frontal GBM. Source: Figure by authors.

Glioblastoma is indicated by the presence of a ring-like enhancement surrounding irregularly shaped regions of putative necrosis. However, non-enhancing tumours such as anaplastic astrocytomas and even glioblastomas might present as non-enhancing lesions at first, especially in elderly patients. Furthermore, low-grade gliomas might sometimes show contrast enhancement. In high-grade malignancies, fluorodeoxyglucose positron emission tomography (FDG-PET) is efficient in revealing hypermetabolism. FDG uptake has long been known to have predictive value. Anaplastic transformation is diagnosed by high FDG uptake in previously known low-grade tumours (Padma et al. 2003). Anatomical imaging is unable to determine tumour margins, which is one of the fundamental drawbacks of using imaging for treatment planning. On both contrast-enhanced T1W MRI and T2W MRI, the tumour expands beyond the margin, according to post-mortem and biopsy studies (Price et al. 2006).

3.1.4. Principles of Glioma Surgery

Glioma surgery aims for the greatest safe resection possible. The surgical removal of these intrinsic brain neoplasms is difficult because they often invade eloquent parts of the brain and lack a distinct border. Preoperative investigations that support anatomical and functional tumour characterization, which aids in defining tumour extent and determining the viability of total resection, are the primary emphasis of this subsection. We also describe intraoperative adjuncts that aid in identifying tumour-infiltrated areas during surgery in order to maximize the extent of resection. Furthermore, the danger of postoperative neurological deficits is reduced while enabling optimal tumour removal with intraoperative functional cortical and subcortical mapping and monitoring. To achieve surgical

objectives and guarantee the best possible patient outcomes, it is advised to combine the use of various modalities both before and during surgery (Krivosheya et al. 2016).

Neuronavigation

Neuronavigation (Figure 3) refers to the localizing techniques that indicate the location of an object in relation to the surgical field sans the need for a fixed, rigid coordinate system, such as a frame firmly affixed to the patient's cranium (Willems et al. 2006). The devising of stereotactic systems that do not rely on stereotactic frames was aided by the convergence of three technological achievements: (1) computers that could manipulate large volumes of MRI or CT data at an acceptable cost and efficiency, (2) improved spatial accuracy (nominally within 1 mm) for CT and MRI during the obtaining of data incorporating the patient's head, and (3) low-cost, accurate 3D digitizers to be used as pointing devices in surgery. Frameless stereotactic neuronavigation thus works by acquiring preoperative imaging data (which will serve as a reference map during the surgical approach and tumour resection), using a localizing tool that will be tracked by the neuronavigation system and will serve as a pointer, and a mathematical framework calculating the relationship between the patient's anatomy and preoperative imaging.

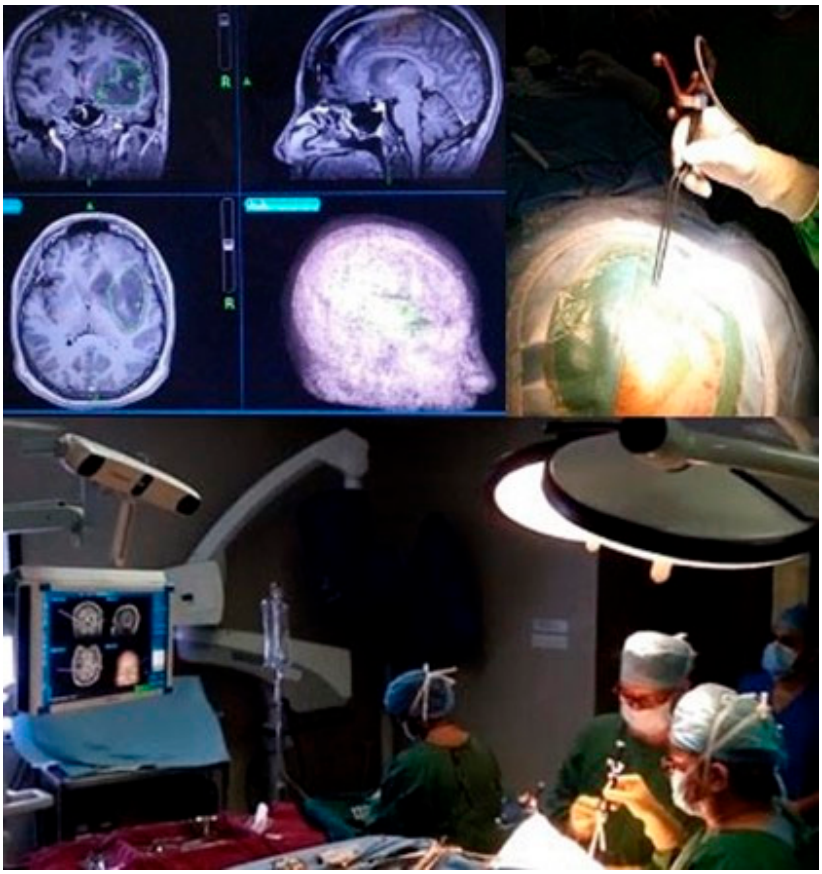

Figure 3. Use of neuronavigation in intrinsic brain tumour surgery (courtesy of Dr. Moududul Haque, Department of Neurosurgery, BSMMU). Source: Figure by authors.

Because there are few, if any, landmarks within the brain's substance, surgical navigation must provide unambiguous guidance to subcortical malignancies. This guidance function is handled in a variety of ways in modern systems. Several research studies have looked at the use of fMRI and DTI for preoperative planning as well as at their intraoperative use as a supplement to surgical navigation for brain tumour removal. It has been found that when fMRI data are paired with DTI data, the accuracy and ability to identify functional structures improves (Kleiser et al. 2010).

Since the 1980s, intraoperative ultrasonography (Figure 4) has been employed for neurosurgery procedures. Intraoperative ultrasonography produces real-time images, has been shown to be helpful in tumour resection, and is faster and considerably cheaper than other intraoperative modalities, such as MRI. Image-guided ultrasonography, which combines the real-time ultrasonographic data with preoperative imaging data, allows

for better interpretation of ultrasound images and improved orientation with the use of the ultrasound probe (Miller et al. 2007).

Figure 4. Intraoperative ultrasonography helps in localizing and resecting tumours in real time. Source: Figure authors.

One of the limitations of conventional surgical navigation is decreased accuracy, especially during the final stages of resection, due to tissue deformation and brain shift caused by changes in tumour volume, CSF drainage, intracranial pressure, brain retraction, etc. (Sherman et al. 2011). Intraoperative MRI can be useful in identifying residual tumour, thus allowing for further resection and improved outcomes of gross total resection. Kubben and colleagues concluded that based on available published studies, there was at least level 2 evidence that iMRI-guided surgery was more effective than conventional navigation with respect to their chosen endpoints in patients with glioblastoma (Kubben et al. 2011). But the benefit of iMRI has to be balanced against its significant cost, which remains its main limitation.

Intraoperative Neuromonitoring

Perioperative neuromonitoring (Figure 5) is critical for guiding surgery and perhaps improving neurologic outcomes by minimizing complications. Clinical neurological examination with a co-operative and awake patient is commonly considered the gold standard of neuromonitoring.

According to the International 10–20 electrode placement system, electroencephalography (EEG) can be monitored using electrodes placed on the scalp. During cerebrovascular surgery, EEG is frequently utilized to detect burst suppression. Nonconvulsive seizures can also be diagnosed with intraoperative EEG monitoring. Electrocorticography (ECoG) produces electrical brain signals that have a high signal-to-noise ratio, are less susceptible to artefacts than EEG, and have a high spatial and temporal resolution. Perioperative ECoG is conducted by placing a specific electrode array on the surface or within the material of the brain utilizing strips, depth, or grid electrodes. It is utilized not only to guide the location of the epileptogenic area, but also to examine the extent to which the seizure focus has been resected.

From the point of stimulation along the neural pathway to the response elicited, evoked potentials assess the central nervous system's integrity. Somatosensory evoked potentials (SEPs), brain auditory evoked responses (BAERs), motor evoked potentials (MEPs), and visual evoked potentials (VEPs) are the commonest of these. When the structures that generate the signal are indirectly or directly at risk owing to damage to or disruption in blood supply, SEP monitoring is used. During neurovascular surgery, MEPs are frequently used. The brainstem component of the auditory evoked response is highly resistant to the effects of anaesthetic medicines, and it is used to assess the integrity of cranial nerve VIII following surgery for acoustic schwannoma as well as other cerebellar pontine angle neoplasms. Because VEP monitoring is more technically difficult, it is not routinely used in the operating room. Intraoperative cortical mapping is commonly utilized to locate the motor strip, sensory cortex, or speech centres for surgery in and around these expressive areas. These procedures necessitate an awake patient, with the operation performed under local anaesthetic with sedation.

Patients with intracranial pathology like severe traumatic brain damage, subarachnoid haemorrhage, intracranial tumours, and cerebral oedema may have an elevated ICP. The importance of early detection and

treatment of increased ICP cannot be overstated. ICP management has the ability to influence outcomes, especially when care is targeted, personalized, and supported with information from other monitors.

Monitoring cerebral oxygenation with jugular venous oximetry allows for the determination of intraoperative cerebral desaturation and guides anaesthetic interventions like optimizing hyperventilation therapy and managing perfusion pressure, oxygenation, and fluids to optimise cerebral physiology. Transcranial Doppler (TCD) ultrasonography is a non-radioactive, non-invasive, and portable technology that uses a range-gated, pulsed Doppler ultrasound to deliver continuous real-time data about cerebral circulation.

Figure 5. Intraoperative neuromonitoring. (**A**) Facial nerve monitoring in cerebellopontine angle surgery. (**B**) Cortical stimulation in awake patient in glioma surgery. Source: Figure by authors.

Intraoperative Dyes

Intraoperative dyes prove useful in several instances in neurosurgery. They are used in CSF leakage and tumour identification, and also in intraoperative angiography (Raza et al. 2016).

Fluorescein has been used intrathecally to detect CSF leaks; however, it has been linked to seizures in some cases. Fluorescein has also been used intravenously to help identify parts of the brain where the blood–brain barrier (BBB) has been broken, such as in malignancies. During the excision of AVMs, it has also been utilized to perform intraoperative "visible angiograms." Intraoperative angiography is performed using indigocyanine green (ICG). It can be seen in regular light or, in some cases, using near-infrared illumination for a better view. This can only be used on surface vessels. With thick-walled atherosclerotic arteries, or big or wide-neck aneurysms, it may be less reliable (Greenberg 2010).

When tumour cells take up nonfluorescent 5-ALA, it causes the production and accumulation of fluorescent protoporphyrin IX (PpIX). Due to a broken BBB, enhanced neovascularization, and overexpression of membrane transporters in malignant tissues, there is greater ALA absorption in brain tumours. PpIX, which is collected selectively in malignant tissue, generates a red-violet light after being excited with blue light generated from a specific filter attachment on the operational microscope, allowing the surgeon to resect red-violet tumour tissue in a gross total fashion (Belykh et al. 2020).

3.1.5. Treatment Considerations

There are some important prognostic factors which are associated with outcomes in patients with LGGs. Clinically, older age, the existence of neurological impairments or a seizure-free state at the outset, and a low performance status (KPS 70%) are all linked to worse outcomes. There is a negative association between tumour volume and overall survival (OS); also, tumour extension to or location in eloquent areas is associated with shorter OS. Speed of growth, expressed as velocity of diametric expansion (VDE)—a measurement reflecting both initial tumour volume and the increase in volume—has been observed to be an independent prognostic factor for OS and malignant-progression-free survival (PFS) (Pallud et al. 2012). Finally, although overall survival broadly correlates with each histological diagnosis, there is extensive evidence that tumours from individual patients who share the same histological diagnosis do not necessarily share the same biology, and their outcomes may vary widely. The limitations of histological diagnosis prompted the search for more clinically relevant markers for stratifying patients with LGGs. Indeed, a number of glioma-relevant molecular markers have been discovered and seem to be superior to histology in predicting outcomes. These include the presence of mutations of the IDH1 or IDH2, ATRX, and TERT genes and the loss of 1p/19q chromosomal arms. They have been incorporated, for the first time, in the latest WHO classification.

Although the importance of surgery in the management of LGGs was once questionable, in all recent series with objective postoperative evaluation of the extent of resection (EOR) based on the volumetric assessment of FLAIR MRI, a considerable improvement in OS was predicted by the degree of resection. This oncological benefit must be, however, balanced against the risk of functional deficit that may arise from radical surgery (onco-functional balance). Advances in the understanding of the brain, tumours, and brain–tumour interactions, as well as the popularization of awake surgeries and direct electrical brain stimulation (DEBS) techniques, have led to improvements in surgical techniques and to a consequent reduction in permanent neurological deficits to below 5% (Duffau et al. 2008). As a result, the primary therapeutic option to explore in LGGs is maximal and early surgical resection. Needle biopsy is only used in individuals who do not want or are unable to undergo surgery due to medical causes. When subtotal resection is not possible, biopsy may be considered for diffuse tumours such as gliomatoses.

The medical management of the symptoms and signs of malignant glioma accounts for a large part of patient care. When treating these individuals, clinicians should keep in mind that the most prevalent issues are peritumoural oedema, seizures, exhaustion, venous thromboembolisms, and cognitive impairment, all of which should be addressed.

The aims of surgery are to obtain a representative tissue sample of the neoplasm for histological and molecular marker assessment as well as to safely remove the tumour with the aim of improving pressure symptoms, improving the efficacy of adjuvant therapy, delaying deterioration, and improving survival; finally, there is the potential of applying surgically delivered treatments (Figure 6). Although no level 1 data are currently available, modern series that utilize exact volumetric measurements of postoperative neoplasm volume seem to support the benefits of increasing the extent of resection (EOR) on progression-free survival (PFS) as well as on OS. A meta-analysis of 37 retrospective studies covering 41,117 unique patients revealed increased chances of survival after gross total resection (GTR) as an analogy to subtotal resection (STR) (Brown et al. 2016). The difficulty in performing the GTR of these tumours is identifying the limits of resection. As there is a poor margin between the tumour and the normal brain, most studies suggest that a GTR is performed in less than 30% of patients (Albert et al. 1994; Kowalczuk et al. 1997). A variety of tools have been developed to improve this resection rate. Image guidance is essential for planning craniotomies, but unpredictable brain shift restricts its use in identifying tumour limits. Intraoperative ultrasound is a useful method, but it is user-dependent. Intraoperative MRI provides the most accuracy, but it is very expensive and does add time to tumour resection (Mehdorn et al. 2011). 5-aminolevulinic acid (5-ALA) fluorescence guiding is a new surgical adjuvant that uses blue (400 nm) light to locate glioma tissue. In cases of malignant glioma, the administration of 5-ALA permits more thorough removal of contrast-enhancing neoplasms, resulting in greater progression-free survival (Stummer et al. 2006). The oncological neurosurgeon's main task is to resect as much as possible while avoiding any neurological damage. Intraoperative function mapping, employing cortical as well as subcortical mapping, has been shown to decrease the risk of postoperative neurological impairments by half (De Witt Hamer et al. 2012).

Adjuvant therapy for high-grade gliomas has traditionally relied on radiotherapy. The evident tumour is defined as gross tumour volume (GTV) in radiotherapy planning. The clinical target volume (CTV) is then estimated by adding a 2.5 cm margin. To generate the planning target volume (PTV), a 0.5 cm buffer is added to

accommodate set-up faults and patient movement. To put it another way, a 3 cm margin is applied around the tumour to protect the normal brain. The dose is thus reduced to decrease the risk of radiation necrosis. In HGGs, two types of radiation are commonly employed. Short-course or palliative radiation delivers a 30-gray dose in six fractions over two weeks, whereas radical radiotherapy delivers a 60-gray dose over thirty daily fractions plus temozolomide during and after radiotherapy (this is known as the Stupp protocol) (Stupp et al. 2005).

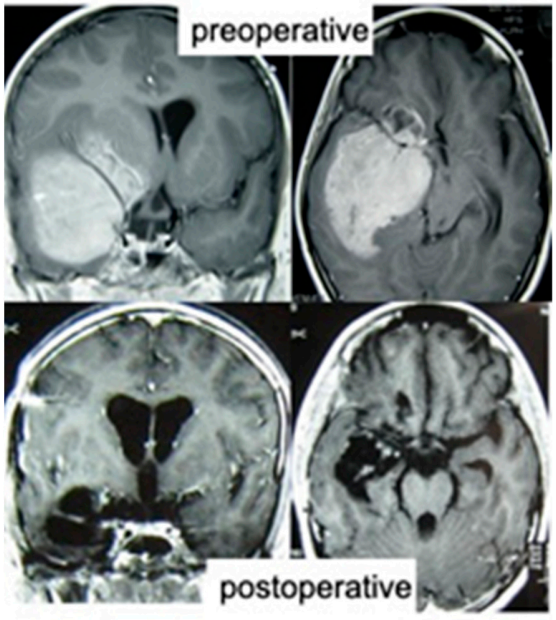

Figure 6. Upper row: preoperative contrast MRI showing right temporal glioma; histology reported GBM. Lower row: contrast MRI six months after the operation and four months after radiotherapy, showing no residual or recurrent tumour. Source: Figure by authors.

The role of chemotherapy as an adjuvant therapy to radiotherapy has been studied in a number of randomized controlled trials. In 2005, a single trial compared the utilization of radiation alone (XRT) to the combination of radiation plus six concurrent cycles of adjuvant temozolomide (XRT/TMZ). Patients who received XRT/TMZ lived an average of two months longer than those who only received XRT. TMZ has a major advantage in that it may be taken orally, and it has quickly become the cornerstone of HGG treatment (Stupp et al. 2005).

In practice, many neurosurgeons use the older classification of gliomas, i.e., low-grade astrocytoma, anaplastic glioma, and glioblastoma multiforme (GBM).

"Low-Grade" Astrocytoma

A total of 5% of all adult primary cerebral tumours are grade 1 or 2 astrocytomas. The average age at which the more common grade 2 tumours arise is 35 years. They consist of well-differentiated astrocytic cells that are further separated into fibrillary, protoplasmic, and gemistocytic types. They are diffuse and grow slowly. The p53 gene is lost in up to 90% of cases. These tumours lack a clear boundary or capsule and extensively invade the surrounding brain, despite being benign.

In children and young adults, pilocytic (grade 1) astrocytomas can develop in the brainstem and cerebellum, in the optic nerve in connection with NF1, and in the hypothalamus. They can frequently stabilize, even regress, and grow extremely slowly.

These may remain asymptomatic for long period. Epilepsy is the most common presentation. Dysphasia, limb weakness, and personality changes can occur over long periods of time. MRI is the investigation of choice and may need to include DTI, tractography, spectroscopy, and fMRI. MRI usually shows a hypointense, non-contrast-enhancing mass in T1W images without or with minimal surrounding oedema.

The excision of low-grade astrocytoma from non-eloquent areas can achieve very good long-term results. However, in eloquent areas, a "safe subtotal/partial resection" of these tumours is performed using awake craniotomy, neuronavigation, brain mapping, or the Duffau concept to avoid neuro-deficits.

About 40% of individuals with grade 2 astrocytomas survive for ten years, and around 50–60% survive for five. Eighty percent of individuals with pilocytic (grade 1) astrocytomas live for twenty years or more (Lindsay et al. 2011).

Glioblastoma Multiforme (GBM)/Anaplastic Astrocytoma

Of all primary cerebral tumours, anaplastic astrocytomas (grade 3) and glioblastoma multiforme (grade 4) account for up to 20%. Anaplastic astrocytoma is four times less prevalent than glioblastoma. The median age upon diagnosis is 45 years old, compared to 64 years old for glioblastoma. These tumours spread widely over the surrounding brain and grow quickly. Histology at autopsy frequently shows dissemination to several distant sites.

Genetic analysis distinguishes between "secondary" glioblastomas, which progress from lower-grade tumours (loss of p53, overexpression of PDGFR, loss of heterozygosity of 10q, abnormalities in the p16 and Rb pathways), and "primary" glioblastomas, which arise de novo (e.g., amplification of EGFR gene, loss of p16, mutation of PTEN, and loss of heterozygosity of 10q).

Clinical presentation includes raised ICP, limb weakness, dysphasia, personality changes, seizures, etc. Clinical features develop gradually, progressing over weeks, months, or years. Sudden deterioration indicates haemorrhage from the tumour. A patient with long-standing epilepsy may experience a quick onset of new symptoms due to a malignant alteration within a "low-grade" lesion. MRI is the investigation modality of choice and may need to include DTI, tractography, spectroscopy and fMRI. MRI usually shows a mixed-intensity (in T1W images) lesion which may be irregularly contrast-enhancing, with surrounding oedema.

Surgery is the mainstay treatment, along with postoperative radiotherapy. Concomitant chemotherapy with radiotherapy is added in GBM patients. The concept of surgical resection is "maximal safe resection". In order to help localize the tumour and assess the extent of tumour removal as the procedure goes on, neuronavigation (frameless stereotaxy), neuromonitoring, or, if possible, real-time CT, MRI, or ultrasound, are frequently used in conjunction with tumour resection. By means of a craniotomy, the physician extracts as much tumour tissue as is safe during an "open" biopsy conducted under direct eyesight. The challenge is that there is no plane of cleavage between the brain and the tumour tissue. The resolution of the imaging limits neuronavigation's ability to identify the boundaries visible on CT or MRI scans. In cases when eloquent regions are nearby, the surgeon may combine tractography or fMRI with the neuronavigation image with or without awake craniotomy to aid in guiding the excision; however, reliability in this regard is still being investigated. An irreparable neurological deficit could be reduced by carrying out the surgery on an awake patient and monitoring the direct effects of electrical stimulation. Large resections in the non-dominant temporal lobe, occipital, or frontal lobes are most securely executed. Most people think that the more cytoreduction—or reduction in tumour bulk—there is, the more effective adjuvant therapy will be.

Although survival has increased due to modern treatments, these tumours still have a poor prognosis. It is impossible to remove everything completely; interhemispheric spread causes even the powerful "hemispherectomy" to fail.

Extensive tumour excision alone increases average survival in surgical patients by only two months; however, when paired with concurrent chemotherapy and radiation therapy, this benefit is increased by an additional twelve months. A total of 25% of patients with this treatment live for two years; more than 40% of patients who have the MGMT gene silenced by promoter methylation survive for more than two years (Lindsay et al. 2011).

3.2. Ependymomas

3.2.1. Clinical Considerations

Ependymomas account for 3–5% of all CNS tumours in adults and almost 10% of all CNS tumours in children. Radial glial cells—bipolar progenitor cells that are thought to be a main source of neurons in the developing nervous system—are hypothesized to be the origins of ependymomas. Ependymomas can occur anywhere along the neuro-axis; they are more frequent in the posterior fossa in children, and in adults, they are more common as intramedullary spinal cord tumours. Previously, it was thought that they came from the lining of the central canal of the spinal cord or the cerebral ventricles; however, recent research suggests that radial glial stem cells may be the source (Taylor et al. 2006). Ependymomas are classified as grade 1 (subependymoma or myxopapillary; though some believe that these are different entities than grade 1), grade 2 (ependymoma with definitions of cellular, clear-cell, papillary, or tanycytic), and grade 3 (anaplastic ependymoma).

The clinical appearance of ependymomas varies according to their size, location, and histologic grade. Hydrocephalus, cranial nerve impairments, and cerebellar dysfunctions are all symptoms of infratentorial ependymoma. Supratentorial extraventricular lesions may present with seizures and focal neurological deficits (e.g., hemiparesis, visual field defects, speech difficulty, behavioural changes, memory deficits); lateral ventricular lesions may present with hydrocephalus and focal neurological deficits; and third ventricular lesions with hydrocephalus, focal neurological deficits, or Parinaud's syndrome (Vellimana et al. 2017). There are no conventional staging criteria for ependymomas. The work-up of patients with suspected ependymoma should include a detailed history as well as a physical examination, followed by MRI of the entire neuro-axis.

3.2.2. Investigative Considerations

On computed tomography (CT) scans, ependymomas may be isodense or hyperdense to the brain parenchyma. Nearly half of these tumours show calcifications, which appear as hyperdense regions on CT. On contrast-enhanced CT scans, these tumours usually demonstrate varying degrees of enhancement that may be heterogeneous; they sometimes enhance homogeneously (Yuh et al. 2009). These MRI appearances are not unique to ependymoma (Figure 7), but they are most often iso/hypointense on T1 sequences, high-signal on T2 sequences, and enhance avidly after contrast. FIESTA (fast imaging employing steady-state acquisition) sequences may allow for more accurate resolution of cranial nerves and vascular structures, and both diffusion-weighted imaging (DWI) and apparent diffusion co-efficient (ADC) mapping are now routinely used to identify high-grade tumours. MRS may also be useful with ependymomas showing a low NAA/choline ratio somewhere between that of a PNET and a glioma. A particular imaging feature which is strongly suggestive of ependymoma is when the tumour fills the lateral recesses of the fourth ventricle or even extends out through the foramina of Luschka and Magendie into the cerebellopontine angle (CPA) and spinal canal, respectively (Chandler 2019).

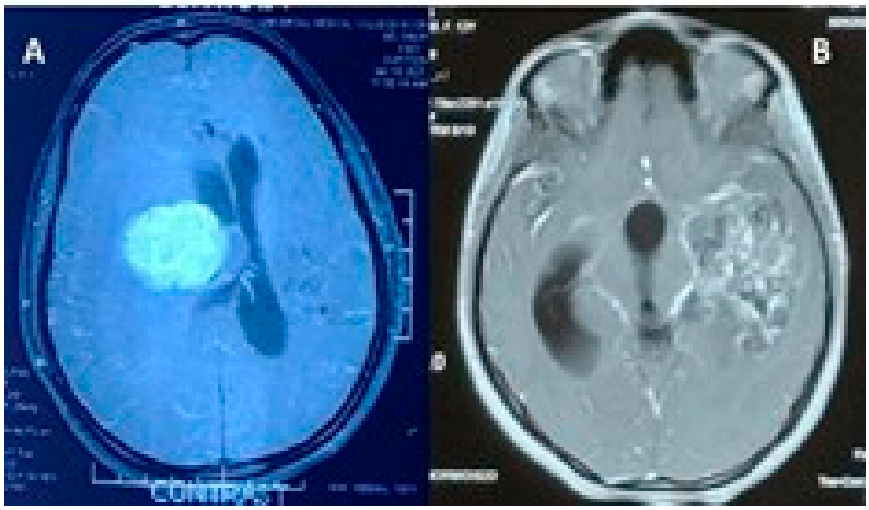

Figure 7. (**A**) Supratentorial extraventricular ependymoma. (**B**) Ependymoma in temporal horn of left lateral ventricle with hydrocephalus. Source: Figure by authors.

3.2.3. Treatment Considerations

The optimal surgical approach for ependymoma is dependent on tumour location (Figure 8).

Infratentorial tumours may be accessed via a standard midline suboccipital craniotomy/ craniectomy and for more lateral tumours, a retromastoid craniotomy/craniectomy may be used. If a pre-resection CSF drainage procedure has not been undertaken, the surgeon might initially create a posterior burr hole and insert an external ventricular drain (EVD) immediately before undertaking the craniotomy. Many neurosurgeons use a telo-velar approach to access fourth ventricular tumours to avoid/minimize damage to the vermis and to try and reduce the risk of posterior fossa mutism/syndrome (Chandler 2019). The aim is always to achieve gross total resection given its paramount importance in prognosis and outcome. Ependymomas are frequently adherent to the brainstem and cranial nerves in the CPA and avoiding damage to these structures can challenge even experienced surgeons. For intraventricular supratentorial ependymomas, an open microsurgical or endoscopic approach can be used. When an open microsurgical approach is chosen, the route commonly includes a trans-sulcal or

transcortical or interhemispheric transcallosal corridor for third ventricular lesions (Geffen et al. 1980). For obstructive hydrocephalus caused by posterior fossa, aqueductal, or posterior third ventricular ependymomas, endoscopic third ventriculostomy and biopsy of the intraventricular lesion are a good therapeutic option, provided the interpeduncular cistern is not obliterated by tumour or brainstem displacement (Vellimana et al. 2017).

Craniospinal irradiation (CSI) as an adjuvant therapy has now been replaced by conformal radiotherapy, which uses 3D imaging and software to optimize dose delivery unless metastatic disease is present (Merchant et al. 2009). A range of different radiotherapy paradigms are now available, including hyperfractionated accelerated radiotherapy, IMRT (intensity-modulated radiotherapy), LINAC, SRS (stereotactic radiosurgery), and proton beam radiotherapy.

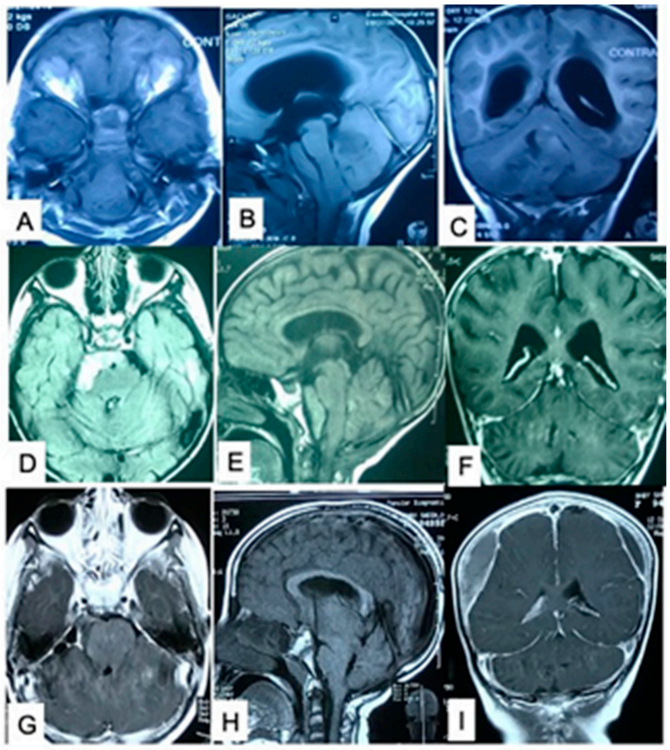

Figure 8. (**A**–**C**) Preoperative contrast MRI of brain showing posterior fossa extraventricular grade 2 ependymoma (non-contrast-enhancing) in a 4-year-old girl. (**D**–**F**) Postoperative (subtotally resected and shunted) contrast MRI of brain showing prepontine and premedullary contrast-enhancing residual tumour 3 months after operation. (**G**–**I**) Postoperative contrast MRI of brain showing no tumour (but there is bilateral parietal asymptomatic subdural effusion) 5 years after operation and adjuvant chemo–radiotherapy. Source: Figure by authors.

3.3. Medulloblastoma

3.3.1. Clinical Considerations

Although medulloblastoma (MB) is a rare disease in adults, accounting for about 1% of all CNS tumours, it is the most prevalent malignant CNS neoplasm in children (Jukich et al. 2001). MB has four different molecular variations, according to the current genomic method. Wingless (WNT), sonic hedgehog (SHH), group 3, and group 4 are the major molecular groupings of MB, with each group having distinct demographics, genetics, recurrence patterns, and outcomes (Northcott et al. 2011). MB is a grade 4 tumour with five variations: classic, desmoplastic nodular, extreme nodular medulloblastoma, anaplastic, and large-cell (Louis et al. 2007). The presenting symptoms and signs depend on the patient's age. Obstructive hydrocephalus and elevated intracranial pressure are common symptoms of a posterior fossa midline tumour. This would result in macrocephaly and a bulging fontanel in infants and toddlers with open sutures. Poor feeding, irritability, regression of milestones, and vomiting usually follow. Older children typically suffer from morning headache and vomiting episodes which relieve the headache. Symptoms due to direct mass effect depend on tumour location. Midline lesions cause truncal ataxia and long tract signs, while more lateral locations—as seen in older children and adolescents—present with cranial nerve palsy, vertigo, and appendicular ataxia. The most common presenting symptoms in adults are

headache, ataxia/gait disturbance, and nausea/vomiting, followed by dizziness/vertigo (vestibular symptoms) and diplopia (Ang et al. 2008).

3.3.2. Investigative Considerations

Head ultrasound can be utilized as an initial imaging tool for the diagnosis of hydrocephalus caused by posterior fossa tumour in children with open fontanel. Computed tomography (CT) would show a midline cerebellar lesion with surrounding vasogenic oedema and obstructive hydrocephalus. Medulloblastomas are hypercellular tumours and they present as hyperdense lesions on CT. Calcifications can be seen in 22% of the cases and cystic formation in 59% (Poretti et al. 2012). All patients with a posterior fossa tumour should undergo a detailed examination of the head and spine with MRI. The imaging characteristics of medulloblastomas are variable in adults, perhaps more so than in children. Whereas tumour locations are predominantly midline (vermian) in children (Figure 9), they are more frequently lateral or hemispheric in adults. The intense or homogeneous contrast enhancement pattern that is frequent in children may not be as common in adults. Tumour margins may appear less distinct in adult medulloblastoma as well. Adult medulloblastomas may appear hypointense on T1W MRI but variable on T2W MRI. The hypercellularity of high-grade tumours such as medulloblastomas, with a high nucleus/cytoplasm ratio, results in reduced free water and gives a high signal (restriction) on diffusion-weighted imaging (DWI) (Fruehwald-Pallamar et al. 2011).

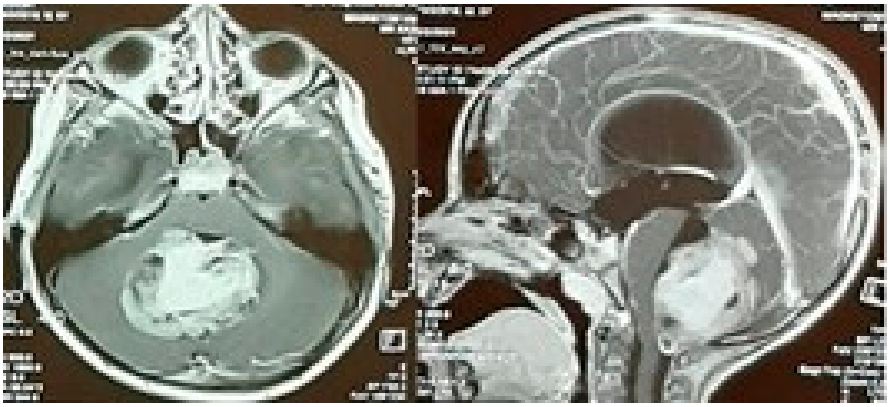

Figure 9. Medulloblastomas are more or less homogenous, highly contrast-enhancing tumours arising from the roof of the fourth ventricle. Source: Figure by authors.

3.3.3. Treatment Considerations

For hydrocephalus due to MB, the routine insertion of ventriculoperitoneal shunts (VPSs) should be avoided because only 10–40% of children will eventually need permanent CSF diversion postoperatively, and these patients will be exposed to a significant risk of VPS complications throughout their lives (Lee et al. 1994). Most surgeons prefer to perform a midline suboccipital craniotomy with the patient in the prone position. Intraoperative neuromonitoring is important. Persistent bleeding usually indicates residual tumour. The endoscope is a useful tool to inspect remnants "around the corners". The target is gross total resection (GTR) under maximum safety. If the tumour invades the floor of the fourth ventricle or is firmly attached to the lower cranial nerves, the surgeon should avoid aggressive resection due to resulting palsies, which significantly decrease the patient's quality of life. According to one study, there is no prognostic dissimilarity between near-total and GTR; hence, there is no need to pursue GTR at the risk of postoperative neurologic morbidity (Thompson et al. 2016).

MB subgroups have various clinical behaviours and may respond favourably to therapies tailored to their particular needs. Norcantharidin, a protein phosphatase inhibitor, has been demonstrated to affect WNT signalling and reduce MB development by promoting nuclear catenin depletion (Cimmino et al. 2011). Smoothened (SMO) inhibitors like vismodegib and sonidegib are the main targets of therapies to modify SHH signalling (Kool et al. 2014). The majority of research on group 3 and group 4 MBs focuses on compounds that block MYC-related pathway activity (Morfouace et al. 2014).

In patients aged under 3 years, even in cases of disseminated disease, current protocols follow radiation-free approaches. In those who are more than 3 years old, adjuvant therapies are stratified into average- and high-risk patients, as per the clinical criteria. Patients in the high-risk group receive 3600 cGy of craniospinal irradiation with

a boost at the tumour bed and to focal metastases. Average-risk patients receive reduced craniospinal irradiation (2340 cGy) with a boost to the tumour bed of 5400–5580 cGy (Gottardo et al. 2014).

3.4. Intracranial Metastasis

3.4.1. Clinical Considerations

Metastatic brain tumours are the commonest brain tumours in adults (Zigouris et al. 2009). Approximately one-third of patients present with a solitary lesion, one-third with oligometastatic (2–3 lesions), and another third with polymetastatic lesions (Norden et al. 2005). The commonest sources of brain metastases in this patient group are cancers of the lung and breast and melanoma, in descending order. In children, the commonest cause of brain metastases is leukaemia, followed by lymphoma (Takakura et al. 1982). Patients with metastases present with signs and symptoms of increased intracranial pressure, CSF pathway obstruction, neurological mass effect, and, in the untreated situation, coning and death. Irritation of the cortex may lead to focal or generalized seizure presentation in 15–20% of patients, but more so (50%) in those with melanoma (Taillibert and Delattre 2005). Solitary or oligometastatic disease presents with headache (80%), focal neurological deficit (30–40%), and visual disturbance (6%), while polymetastatic disease may present as an encephalopathic or acute confusional state (Gaspar et al. 1997).

3.4.2. Investigative Considerations

The grey/white junction is commonly the site of supratentorial cerebral metastases. Sometimes, they are dural-based. There is typically peripheral or heterogeneous enhancement on contrast CT or MRI examination. Brain metastases are frequently accompanied by severe surrounding oedema that is often out of proportion to the size of the tumour. High-grade glioma, subacute infarct, and brain abscess are among the possible diagnoses for ring-enhancing cerebral lesions. These can be distinguished using advanced MRI.

Magnetic resonance spectroscopy (MRS) analysis of malignancies reveals increased choline (CHO) and decreased creatine (CRE) and n-acetyl aspartate (NAA) (Figure 10). Areas of necrosis with higher lactate are frequent in high-grade gliomas, which typically have lower myoinositol levels (Castillo et al. 2000).

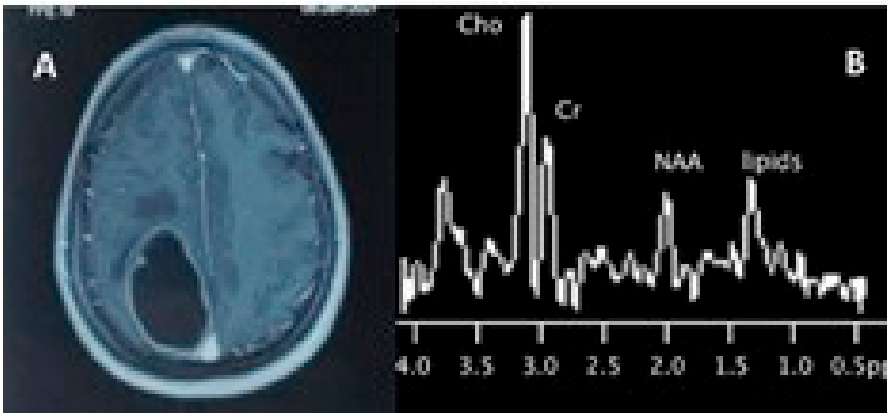

Figure 10. (**A**) Cerebral metastases are usually peripherally enhancing lesions with surrounding oedema which are occasionally dural-based. (**B**) MRS typically shows elevated choline (Cho) and depressed creatine (Cre) and n-acetyl aspartate (NAA). Source: Figure by authors.

3.4.3. Treatment Considerations

High-dose corticosteroids are used in the early stage of the management of patients with symptomatic brain metastases in order to decrease the oedema that classically surrounds these tumours and to help restore neurological function. Individual treatment options can be divided into focal (surgery, stereotactic radio surgery (SRS), interstitial laser therapy, and focused ultrasound treatment) and whole-brain or -body techniques (whole-brain radiotherapy (WBRT), chemotherapy, and targeted or immune therapies). Patient-related factors like age, performance status, the occurrence of extracranial metastases, and the condition of the primary tumour continue to be the key determinants of patient outcome (Gaspar et al. 1997).

The preferred treatment for individuals with a solitary brain metastasis is gross surgical resection, followed by WBRT or SRS to the tumour bed to stop local recurrence and perhaps increase survival. This is especially true for younger patients with stable extracranial illness and a KPS 70. WBRT, along with SRS, offers the best survival benefit in patients with tumours that are inaccessible to surgery, who have several concomitant conditions, have a low KPS, or who choose not to have surgery. However, WBRT may have considerable adverse cognitive effects, and the risk must be balanced with the benefit. Although WBRT remains the standard of care for patients with polymetastatic brain disease, improved planning algorithms have allowed for the use of SRS in these patients. Multiple lesions can be managed with acceptable toxicity due to the sharp dose drop-off and conformity provided by stereotactic systems. According to a recent trial, stereotactic radiosurgery in patients with five to ten brain metastases is not inferior to that in patients with two to four brain metastases when performed without WBRT (Yamamoto et al. 2014). For patients with up to ten brain metastases, stereotactic radiosurgery may be a good alternative because of its low level of invasiveness and favourable side effect profile in comparison to WBRT. In patients with multiple brain metastases (BM), survival following whole-brain radiation therapy (WBRT) is currently predicted using group-based scoring systems that have limited decision-making utility. For the assessment of survival in patients with short life expectancy, however, a more pertinent tailored predictive model can be utilized, such as the Diagnosis-Specific Graded Prognostic Assessment (DS-GPA) or the Radiation Therapy Oncology Group Recursive Partitioning Analysis (RTOG-RPA) (Marchand-Crety et al. 2021).

If surgical intervention is chosen, an en bloc resection technique including dissection just outside or inside the pseudocapsule should be tried. This approach limits the spillage of tumour cells, in addition to meticulously devascularizing the tumour. Piecemeal resection was found to be inferior to this approach (Patel et al. 2009). If the tumour is close to the eloquent cortex, a margin of less than 5 mm is desired but not always possible. As it avoids piecemeal resection, the Cavitron ultrasonic aspirator (CUSA) is frequently useful in achieving this goal.

4. Extrinsic Tumours and Tumour-like Conditions

4.1. Meningioma

4.1.1. Clinical Considerations

Meningiomas were first described by Harvey Cushing in 1922 and have since been recognized as the commonest intracranial nonglial tumour (Ostrom et al. 2016). Meningiomas are thought to originate from meningothelial cells (also known as arachnoidal cap cells). Meningothelial cells are most abundant on the surface of arachnoid villi around major venous sinuses, large cerebral veins, crista galli, and over the basilar venous plexus, but are also found in the arachnoid membrane in all its locations and other parts of the CNS (Haines and Frederickson 1991). In descending order of occurrence, the approximate distribution of intracranial meningiomas is as follows: convexity (35%), sphenoid ridge (20%), parasagittal (20%), intraventricular (5%), tuberculum sellae (3%), infratentorial (13%), and others (4%) (Almefty et al. 2017).

Depending on the location (Figures 11 and 12), meningiomas can produce a wide array of symptoms. Symptoms and signs can be related directly to the compression of adjacent neural structures or secondary to the effects of elevated intracranial pressure. For example, if the tumour is located on the medial part of the sphenoid wing, decreased vision and eye movement paralysis may be commonplace, whereas a tumour at the posterior fossa may give rise to a different constellation of symptoms, including hydrocephalus and dysphonia. As a consequence of the irritation of the cerebral cortex, seizures may occur with supratentorial meningiomas (Birk et al. 2019). WHO recognizes three grades of meningioma on the basis of pathologic criteria and the risk of recurrence and aggressive growth. Diagnosis of atypical (grade 2) and anaplastic (grade 3) meningiomas is made primarily based on mitotic count, regions of hypercellularity, nuclear/cytoplasmic ratio, sheet-like growth, prominent nucleoli, and spontaneous necrosis. However, some rare meningioma subtypes, characterized by particular tumour cell phenotypes, are linked to more common recurrence and are automatically (regardless of the presence of the aforementioned histological "features of malignancy") graded as WHO grade 2 (chordoid and clear-cell) or WHO grade 3 (papillary and rhabdoid) meningiomas (Raza et al. 2016).

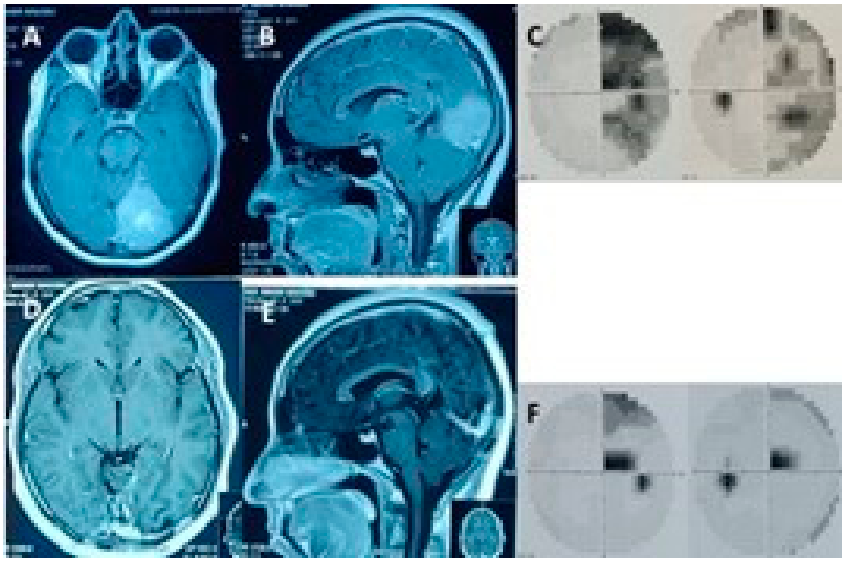

Figure 11. A case of peritorcular meningioma with right homonymous hemianopia (**A**–**C**). Improvement in visual field after tumour excision (**D**–**F**). Source: Figure by authors.

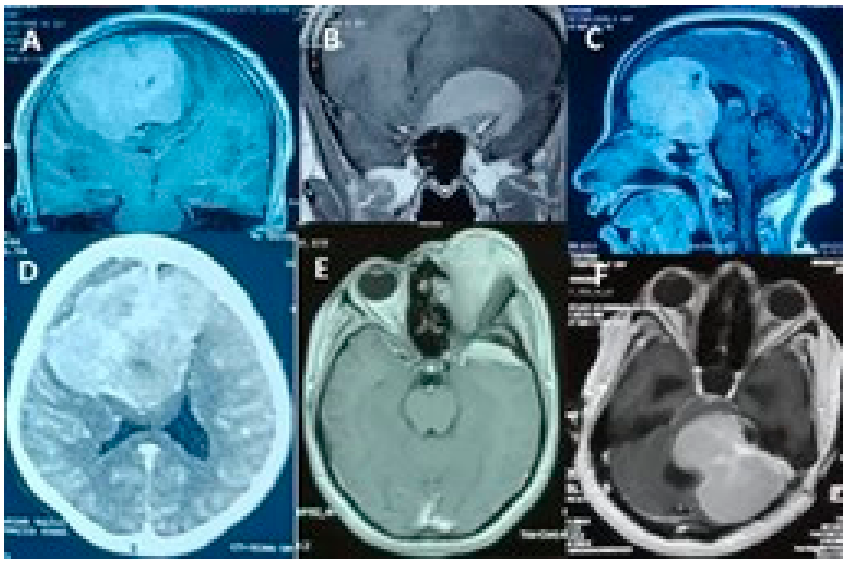

Figure 12. Meningiomas in different locations: (**A**) convexity meningioma; (**B**) clinoidal meningioma; (**C**) olfactory groove meningioma; (**D**) falcine meningioma; (**E**) spheno-orbital meningioma; (**F**) posterior fossa meningioma. Source: Figure by authors.

4.1.2. Investigative Considerations

Patients with meningioma have three distinctive features on plain radiographs: hyperostosis, enhanced vascular patterns, and calcification. Meningiomas often appear isodense to slightly hyperdense on non-contrast-enhanced CT scans in comparison to the contiguous brain parenchyma. There could be calcification. Meningiomas typically grow uniformly and strongly. The tumour usually has a large base and a sharp edge against a bone structure or dural margin. They may appear isointense to the brain on T1W and T2W MRI scans, but gadolinium enhancement is the norm. On T2W images, hyperintensity indicates a meningothelial meningioma, a vascular meningioma, or an aggressive meningioma, all of which have a higher water content. It does, however, point to a tumour that may be removed with ease during surgery. After receiving a contrast agent, the dura mater next to a meningioma's connection may seem enhanced on a CT or MRI scan (Figures 11 and 12). Histological analysis conducted on these alleged dural tails found meningioma cell nests, despite some cases only exhibiting connective tissue and vascular tissue development (Nakau et al. 1997).

DSAs (digital subtraction angiograms) are another tool used in diagnosis. The tumour contrast blush comes early (in the arterial phase), persists late (beyond the venous phase), and is quite thick. Usually, the external carotid artery serves as a feeder for meningiomas. Venograms are only performed to evaluate the dural venous sinuses when treating a parasagittal meningioma, and angiograms are only performed when preoperative embolization would be advantageous (Alalade and Kitchen 2018).

4.1.3. Treatment Considerations

In meningioma surgery, Simpson grading is used to level the extent of excision.
Simpson grading (Simpson 1957) is as follows:

Grade 1—macroscopically complete tumour resection with excision of involved dura and bone.
Grade 2—macroscopically complete tumour removal with coagulation of involved dura only.
Grade 3—macroscopically complete tumour removal without removal of involved dura and bone.
Grade 4—subtotal tumour resection.
Grade 5—decompression with or without biopsy.

Complete surgical resection is the only effective form of management for meningioma (Figures 13–16). Less likelihood of recurrence exists with more thorough excision. Simpson established a five-grade system for categorizing meningioma surgery in 1957. The recurrence rate for grade 1 is about 10%, while it is twice as high for grade 2. It is understandable that the rates of recurrence are higher in the higher Simpson grades. Grade 0 removal is defined as the addition of a 2 cm dural margin.

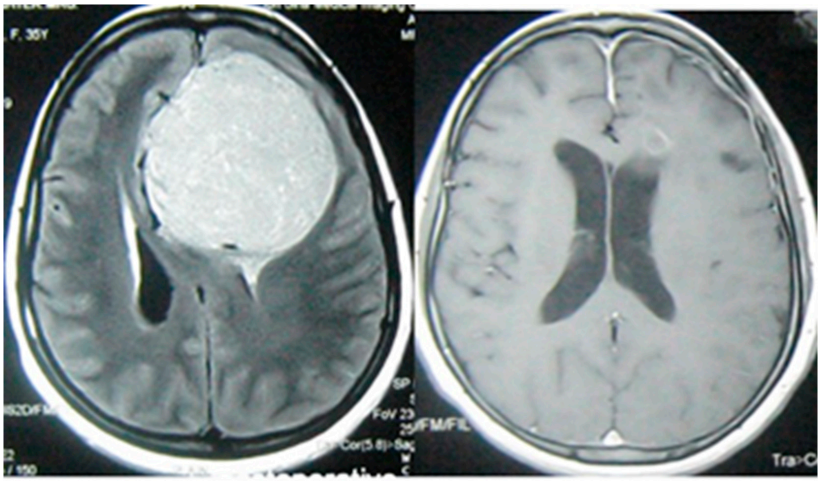

Figure 13. Contrast MRI of brain axial sections; left side shows huge preoperative anterior falcine meningioma and right side shows postoperative complete excision of meningioma. Source: Figure by authors.

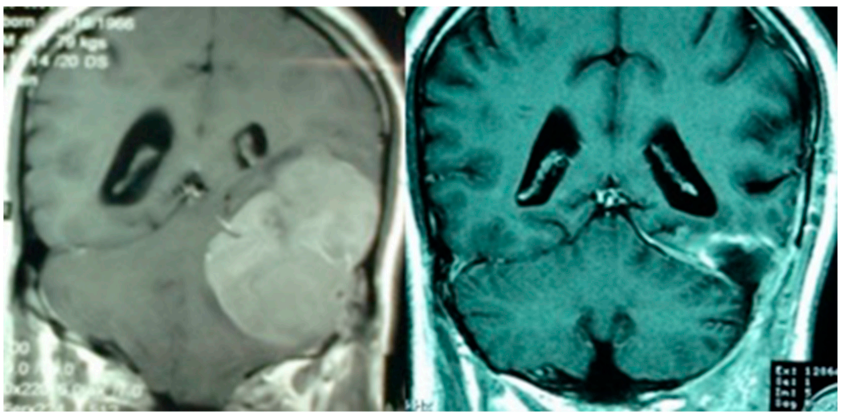

Figure 14. Contrast MRI of brain coronal sections; left side shows huge preoperative tentorial meningioma and right side shows postoperative complete excision of meningioma. Source: Figure by authors.

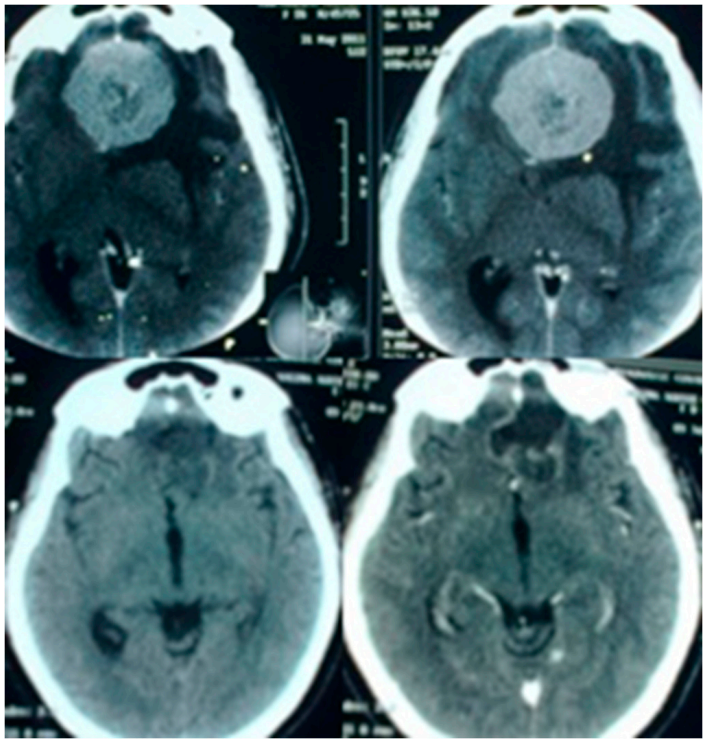

Figure 15. Contrast CT scan of brain axial sections; upper row shows preoperative olfactory groove meningioma, and lower row shows postoperative complete excision of meningioma. Source: Figure by authors.

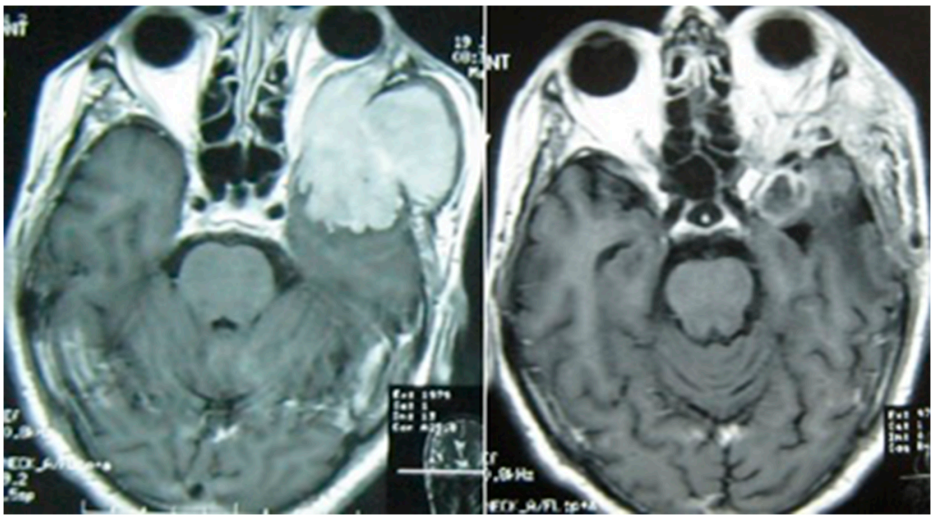

Figure 16. Contrast MRI of brain axial sections; left side shows huge preoperative anaplastic sphenoidal wing meningioma, and right side shows postoperative complete excision of meningioma. Source: Figure by authors.

While surgical resection is the preferred course of treatment, radiation therapy (Figure 16) should be taken into consideration in the following situations: (1) following surgery for a malignant meningioma; (2) after incomplete excision of a meningioma for which the risk of excision of a later recurrence is judged to be excessive; (3) for patients with multiple recurrent neoplasms for whom the surgeon finds that repeat surgery will be very hazardous; and (4) as the only therapy in a patient with progressive symptoms (Guthrie et al. 1991).

Given the relative ease of access, Simpson grade 1 or even grade 0 resection should be conducted in convexity meningiomas. When the bone is involved, removal of the hyperostotic bone with a healthy margin and of the pericranium in an en bloc resection is recommended (Kinjo et al. 1993).

Parasagittal meningioma arises from the dura of the superior sagittal sinus (SSS). The superior sagittal sinus is often not involved in falcine meningioma, which develops from the falx and may be totally hidden by the overlying cortex (Cushing and Eisenhardt 1938).

The most crucial decision in the treatment of parasagittal and falcine meningiomas is selecting the best way to handle the affected sinus. In these situations, a very useful preoperative adjunct may be an MR venogram (Asari et al. 1995). The patient's age and symptoms, patency of the sinus, the site and side of the tumour, and the cerebral venous collateral system should all be taken into account while making decisions about the sinus in each situation (Birk et al. 2019). A sinus that is completely obstructed can be removed at any time. It is crucial for the procedure, and cannot be overstated how important it is, to maintain collateral venous pathways. It is possible to remove the front section of the sinus with or without a graft or replacement. After the tumour has been removed from the sinus, the infiltration of the tumour in one wall can mostly be healed. Early devascularization through interhemispheric exposure along the falx is recommended in falcine tumours when there is a unilateral tumour. To protect the pericallosal arteries in the inferior margin of the dissection and prevent damage to the surrounding cerebral cortex and pial tissue, larger tumours should first undergo central debulking, followed by microsurgical separation of the tumour capsule from the arachnoidal areas (Almefty et al. 2017).

The surgical removal of tentorial meningiomas is based on their specific location. The petrous apex with extension into the perimesencephalic region can be removed utilizing the anterior petrosal approach in malignancies affecting the anterior to midmedial incisural ring. For lesions spreading posteriorly into the lateral pontine region, this method can be used in conjunction with an anterior petrosectomy. The petrosal technique can be used to access lesions that affect the middle-to-posterior portion of the inner ring of the tentorium, as well as the petroclival area and extension into the perimesencephalic cistern (Almefty et al. 2017). A posterior interhemispheric transtentorial technique can be used to access falcotentorial lesions. A supracerebellar infratentorial technique can be used to address tumours at the falcotentorial junction, which are primarily infratentorial (Asari et al. 1995). The supra–infratentorial technique can be used to access larger tentorial leaf tumours with superior extension into the occipital lobe as well as inferior extension into the cerebellum (Sakaki et al. 1987).

For olfactory groove meningioma, a frontal transbasal approach with a supraorbital osteotomy or its modifications allows for the early control of its blood supply, which is predominantly from the anterior ethmoidal artery, and for the placement of a pericranial flap to repair the skull base after cranialization of the frontal sinus and drilling of the hyperostotic bone at its origin (Cusimano and Meier 2019). Tuberculum sellae and planum sphenoidale meningiomas that are small or extend into the sphenoid sinus with an absence of vascular encasement and do not extend laterally to the carotid may be considered for extended endoscopic endonasal approaches (Neil and Couldwell 2019). For others, the pterional approach allows the surgeon to deal with further extensions into the interpeduncular cistern and around the internal carotid artery, but it will likely involve a degree of manipulation of the ipsilateral optic nerve and the area medial to the nerve could be a blind spot. The anterior interhemispheric, rather than subfrontal, approach can preserve olfaction more readily and avoid manipulation of the optic nerves, but a retroclival extension, especially with a prefixed chiasm, is a blind spot (Nimmannitya et al. 2016).

Following extradural drilling of the sphenoid ridge, which also helps to devascularize the tumour, lateral sphenoid wing meningiomas can be removed. After extradural drilling of the sphenoid wing, meningiomas that develop from the middle part of the sphenoid wing are also removed. A cranio-orbital zygomatic craniotomy might be the most effective treatment for malignancies that affect the orbit and superior orbital fissure and progress toward the cavernous sinus (Almefty et al. 2017). The cranio-orbital zygomatic approach can also be used for the resection of clinoidal meningiomas. This offers the surgeon a low-based approach, numerous dissection options, little brain retraction, and, if necessary, the possibility to penetrate the cavernous sinus (Al-Mefty 1991). The larger sphenoid wing, anterior clinoid, superior and lateral orbital walls, and the afflicted dura are all completely removed during surgery for spheno-orbital meningiomas. After carefully repairing the dura with an autologous graft, a cranioplasty is performed for cosmetic purposes (Bikmaz et al. 2007).

According to the description, petroclival meningiomas develop from the top two-thirds of the clivus and from the medial to the trigeminal nerve, at the petroclival junction. Petroclival meningiomas may involve the cavernous sinus through the Meckel cave and cross the middle and posterior cerebral fossae. Sphenopetroclival meningiomas are the most severe ones and invade the sella turcica, sphenoid sinus, and/or cavernous sinus(es) (Alalade and Kitchen 2018). It is debatable which method should be used to remove petroclival meningiomas. Some surgeons like the retrosigmoid approach with the patient in the sitting position, citing its simplicity, while others favour petrosal techniques (Samii and Tatagiba 1992). The transpetrosal partial labyrinthectomy–petrous

apicoectomy approach takes a much longer time to accomplish than the retrosigmoid approach. In these two approaches, the temporal lobe and cerebellum, respectively, are retracted. The transpetrosal approach permits a direct view of the tumour, whilst in the retrosigmoid approach, cranial nerve traction is extensive (Al-Mefty et al. 1988). A trans-zygomatic approach may be used when the tumour involves the upper clivus. Tumours involving the lower and mid-clivus are approached by a presigmoid approach, occasionally with division of the non-dominant sinus (Erkmen et al. 2005). Skull base reconstruction is a must in all approaches to prevent CSF leaks.

4.2. Solitary Fibrous Tumour (Haemangiopericytomas)

4.2.1. Clinical Considerations

Haemangiopericytomas–solitary fibrous tumours (HPC-SFTs) were once classified as meningiomas and haemangiopericytomas (HPCs). Since the 2013 edition of the WHO Classification of Tumours of Soft Tissue and Bone, HPCs and SFTs are considered one entity. The term HPC has been abandoned and both entities are now called SFTs (Fletcher et al. 2013). This is because they share the same NAB2-STAT6 fusion gene. Molecular studies on HPCs of the dura/meninges have detected similar genetic aberrations, and the most recent WHO Classification of Tumours of the CNS also considers haemangiopericytomas–solitary fibrous tumours as the same entity (Louis et al. 2016). HPCs are generally WHO grade 2 and grade 3. Although the ultimate diagnostic test is identifying the NAB2-STAT6 fusion gene, this is not practical as the first step. Instead, identification of nuclear staining of STAT6 using immunohistochemistry is a good surrogate test (Schweizer et al. 2013).

4.2.2. Investigative Considerations

On imaging tests, meningiomas and HPCs may look similar. A thin- or broad-based meningeal attachment is often visible on CT. On unenhanced CT images, the tumours typically appear hyperdense with focal areas of hypodensity, and after the administration of a contrast agent, they show areas of heterogeneous enhancement (Chiechi et al. 1996). More than 50% of haemangiopericytomas exhibit bone erosion. Hyperostosis is not a characteristic of these tumours (Sibtain et al. 2007). On T1- and T2-weighted MRI, haemangiopericytomas typically show large vascular flow voids and are isointense to grey matter. The most frequent appearance on T1-weighted gadolinium-enhanced images is heterogeneous enhancement (Chiechi et al. 1996). The dural tail sign is present in about half of the malignancies. If the diagnosis is of HPC, body staging is conducted, as the frequency of systemic metastases is high (25–50%) (Damodaran et al. 2014).

4.2.3. Treatment Considerations

The surgical excision of an HPC follows similar concepts as that of a meningioma. The main treatment for HPC is surgery, with a goal of a Simpson grade 1 gross total resection. This requires the removal of bone, dura, and, if necessary, brain or vascular structures, provided that doing so will not result in an unacceptable severe neurological loss. Every effort should be made to accomplish total removal during the initial resection, as surgery for recurrent tumour is usually more challenging and less effective. Due to the high vascularity of many HPCs, significant bleeding during surgery is the biggest potential challenge. After surgery, 60–75% of HPC cases return. At ages 5, 10, and 15, metastatic rates are 13%, 33%, and 64%, respectively, according to Guthrie and colleagues (Guthrie et al. 1989). Studies have shown that stereotactic radiosurgery can effectively cure recurrent or residual disease (Chang and Sakamoto 2003).

4.3. Dermoids and Epidermoids

4.3.1. Clinical Considerations

Dermoid and epidermoid cysts, also termed congenital ectodermal inclusion cysts, are commonly derived from retained surface ectoderm trapped by two fusing neuroectodermal surfaces during neural tube closure. Dermoid cysts have a tendency to occur near the midline. The most common intracranial sites are near the anterior fontanelle extradurally and in the sellar, parasellar, and intraventricular regions intradurally. The commonest intraspinal site is near the cauda equina; this localization can be linked to a dermal sinus tract and subsequent increased risk of bacterial infection. Dermoid cysts are composed of epithelial cell debris and keratin and also include elements of the dermis like hair follicles, sebaceous glands, and sweat glands. Epidermoid cysts are mainly

intracranial and are found away from the midline. The commonest site is the cerebellopontine angle (40–50%), where they make up the third commonest lesion in adults after vestibular schwannomas and meningiomas. They are also found in the fourth ventricle, the sellar and parasellar regions, the cerebral hemispheres, and the brainstem. Epidermoid cysts are composed of only epithelial cell debris, including cholesterol and keratin, laid down in a lamellar pattern, with no dermal involvement. Compared to patients with epidermoids, patients with dermoid cysts typically present at a younger age. For dermoid cysts, the average age at presentation is 15 years, while it is 35 years for epidermoids, according to Gormley and colleagues (Gormley et al. 1994). In a study by Love and Kernohan, patients with dermoid tumours experienced symptoms for an average of 8.5 years, compared to those with epidermoid tumours, who experienced symptoms for an average of 16 years (Chowdhury et al. 2013; Love and Kernohan 1936). Symptoms and indicators vary depending on the site of the tumour. Extradural lesions often present as local masses with or without headache (Gormley et al. 1994). Due to their frequent parasellar position, intradural tumours are more frequently linked to headache, visual impairment, and, to a lesser extent, changes in the hypothalamus. While tumours near the cerebellopontine angle may result in ataxia, vertigo, or localized impairments in the cranial nerves, those in the middle fossa grow quite slowly and frequently exhibit no symptoms (Akar et al. 2003). Sometimes, a more acute presentation results from a cyst rupture, which causes the contents of the cyst to flow into the subarachnoid space and cause chemical meningitis. This should be distinguished from the septic meningitis seen in intraspinal dermoid cysts, caused by the presence of a dermal sinus tract. Cyst rupture can lead to several neurological sequelae, including headache, seizures, vasospasm, neurological deficit, and death (Chowdhury et al. 2013; Love and Kernohan 1936).

4.3.2. Investigative Considerations

In epidermoids, the subarachnoid space typically contains a homogeneous, non-enhancing, hypodense lesion without surrounding oedema. Arachnoid cysts are the most problematic cystic tumours, with craniopharyngioma, Rathke's cleft cyst, and other cystic tumours also included in the differential diagnosis. The preferred imaging method for identifying these lesions today is MRI (Figure 17a,b and Figure 18). The tumour signal typically exhibits hypointensity on T1W imaging and hyperintensity on T2W images and is heterogeneous (Kumari et al. 2009). On proton density investigations, a rim of strong signal intensity may be seen; some tumours exhibit rim enhancement after gadolinium injection. The previously described cystic entities are part of the differential diagnosis. On standard and spin echo MRI pulse sequences, it is challenging to distinguish between epidermoids and arachnoid cysts; however, DW, FLAIR, constructive interference in steady state, and fast imaging with steady state precession studies can frequently distinguish between epidermoid tumours (Figure 19) and CSF within arachnoid cysts (Hakyemez et al. 2005). On a CT scan, dermoids are often avascular and hypodense, and they do not exhibit contrast enhancement. Dermoid cysts can have a variable appearance on MRI, depending on the balance of their contents, which may include fat, hair, sebum, and teeth. They differ from lipomas in that they do not feature consistent fat densities on all sequences (Osborn and Preece 2006). Dermoid tumours tend to be more localized and exhibit a greater local mass effect than epidermoid tumours because they are often more solid than epidermoid tumours.

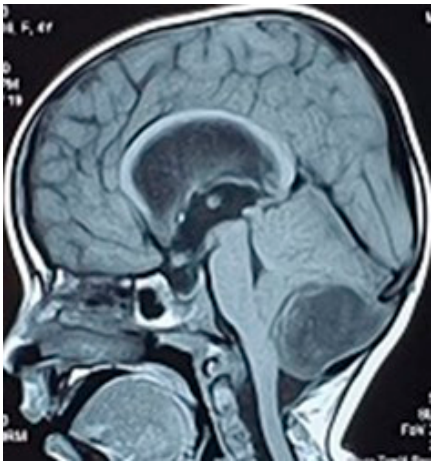

(**a**)

Figure 17. *Cont.*

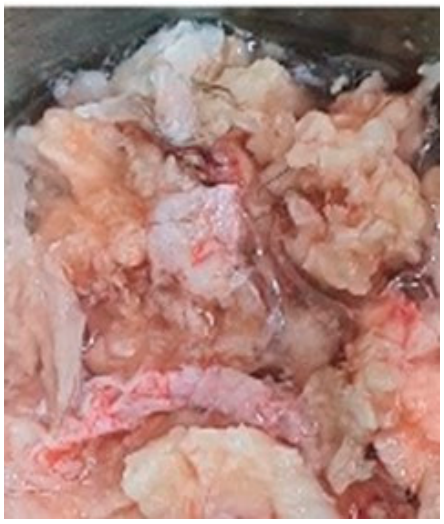

(**b**)

Figure 17. (**a**) Sagittal section of MRI of a child with a posterior fossa dermoid. (**b**) Typical content of dermoid found perioperatively in the patient in. Source: Figure by authors.

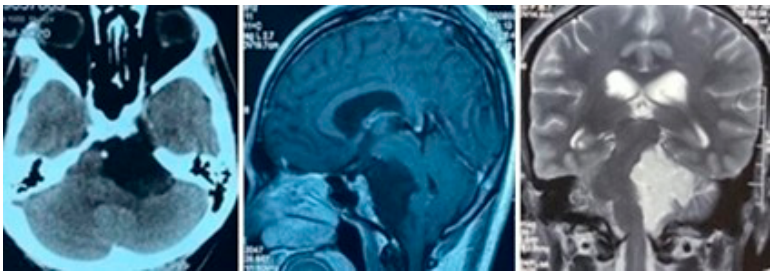

(**a**) (**b**) (**c**)

Figure 18. (**a**) Epidermoids are non-contrast-enhancing irregular isodense lesions along the CSF cisterns in CT images. (**b**,**c**) They also show the same intensity as the CSF in MR images, with DWI being the main differentiating sequence. Source: Figure by authors.

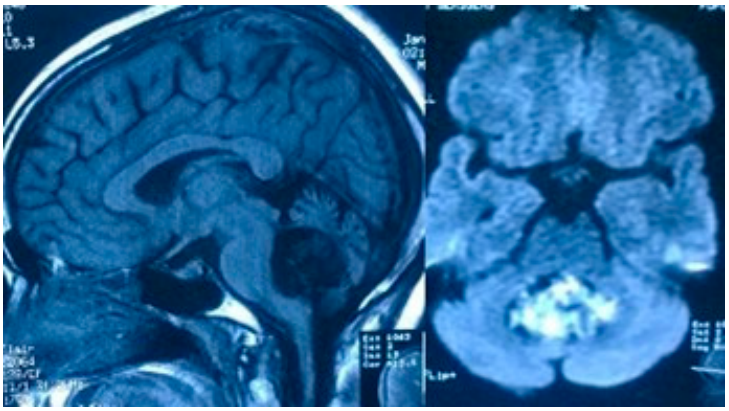

Figure 19. MRI of brain. (**left**) TW1 sagittal image; (**right**) DW axial image showing 4th ventricular epidermoid. Source: Figure by authors.

4.3.3. Treatment Considerations

The main aim of the operation should be the stark removal of the cyst, including the epithelial lining, to provide curative treatment and remove the risk of recurrence. However, surgery can be technically demanding on account of the deep, critical location of the tumours and their relationship to the surrounding neurovascular structures (Gormley et al. 1994). Independent of the surgical approach, resection can be technically demanding for several reasons. Tumour adhesion to adjacent structures on the skull base and also to the surrounding brain parenchyma is common. This is most pronounced with dermoid cysts, which tend to cause a greater granulomatous reaction with the arachnoid mater and occasionally the pia mater. On the other hand, cysts can

extend between different anatomical compartments, which is more pronounced in epidermoid cysts (McEvoy 2019). These cysts contain characteristic pearly flakes (Figure 17) (Hassaneen and Sawaya 2017).

5. Sellar, Suprasellar, and Parasellar Tumours

5.1. Pituitary Tumours

5.1.1. Clinical Considerations

The sella turcica, in which the pituitary gland is located, is an intricate assembly of anatomical structures which include neural, endocrine, vascular, osseous, and meningeal tissues and which are in close relation to the cavernous sinus, hypothalamus, and major blood vessels. Lesions of the sella turcica are diverse and include neoplastic and non-neoplastic lesions. Pituitary adenomas are the most common lesions; these are usually benign tumours and comprise 10–12% of all intracranial tumours. Most of these tumours arise from the anterior pituitary, which comprises 80% of the gland's mass. Pituicytomas are tumours of the neurohypophysis. Both sexes are equally affected. Pituitary adenomas in children are about ten times less common than in adults, contributing to 2 to 6% of all intracranial tumours (Keil and Stratakis 2008). The majority of pituitary tumours are sporadic (95%). A small minority are familial (5%) and occur as either isolated lesions or as part of a familial genetic syndrome like multiple endocrine neoplasia (Vandeva et al. 2010; Marques and Korbonits 2017).

Pituitary tumours have a diversity of presentations, including endocrine syndrome, mass effect, incidental finding, pituitary apoplexy, CSF rhinorrhoea, and headache. Prolactin hypersecretion may occur due to prolactinoma or pituitary stalk syndrome. Growth hormone excess may produce acromegaly in adults and gigantism in prepubertal children. Excess corticotropin may produce Cushing's disease or Nelson syndrome in patients who undergo bilateral adrenalectomy. Thyrotropin excess may cause secondary hyperthyroidism, which is very rare, and FSH- and LH-secreting tumours usually do not result in any clinical syndrome.

The hyposecretion of pituitary hormones may cause pituitary cachexia or Simmond's cachexia. Growth hormone deficiency may cause growth delays in children and vague symptoms in adults. Hypogonadism may lead to amenorrhoea, loss of libido, and infertility. Mass effect is usually caused by non-functioning tumours. They may compress the optic nerve and may cause classical bitemporal hemianopia. Other field defects could be superior temporal quadrantonopia, monocular blindness, junctional scotoma, homonymous hemianopia, and central scotoma. Cavernous sinus compression may cause pressure on cranial nerves III, IV, V1, V2, and VI, as well as causing chemosis and proptosis.

Pituitary apoplexy is a condition where neurologic and/or endocrinologic deterioration occurs due to the sudden enlargement of a mass within the sella turcica due to haemorrhage, necrosis, or infarction of a pituitary adenoma. The patient may present with headache, visual disturbance, ophthalmoplegia, ptosis, Horner's syndrome, and alteration of consciousness level. Hypothalamic involvement may also produce hypotension, thermal dysregulation, cardiac dysrhythmia, respiratory pattern disturbance, altered mental state, and diabetes insipidus (DI). CT scan or MRI reveals a haemorrhagic mass. Urgent management includes endocrine evaluation, rapid administration of corticosteroids, and rapid decompression by surgery.

Prolactinoma is the most common tumour among functioning tumours. It may cause amenorrhoea–galactorrhoea syndrome in female patients and impotence and decrease libido in male patients, as well as infertility and bone loss in both sexes. The most common tumours in the posterior pituitary are metastases, and granular cell tumours are the most common tumours of the neurohypophysis.

5.1.2. Investigative Considerations

For the assessment of a pituitary tumour, it is essential to evaluate the levels of all anterior pituitary hormones, like growth hormone, prolactin, ACTH, TSH, LH, and FSH. It is also important to assess morning and evening cortisol levels, insulin-like growth factor 1 and blood sugar levels, and HbA1c and testosterone levels. Formal visual assessment gives details of visual impairment, which are particularly important for macroadenoma. Acromegaly patients may have high growth hormone as well as insulin-like growth factor 1 levels. Cushing's syndrome patients may have hyperglycaemia, loss of diurnal variation in cortisol level, hypokalaemic alkalosis, increased 24-h urine free cortisol, and a positive dexamethasone suppression test.

A plain X-ray of the skull gives little information about pituitary tumours, but is sometimes required for documentation; in acromegaly patients especially, X-ray of the skull, hands, and feet is required. CT scan of the brain with contrast gives information regarding tumour details, contrast enhancement, micro- or macroadenoma,

haemorrhage, and calcification. MRI of the brain is the diagnostic investigation of choice and gives the complete picture of tumour details (Figure 20).

On T1WI, the posterior pituitary shows high signal, also referred to as the "bright spot". Tumours are usually hypointense in T1WI and hyperintense in T2 WI. Sometimes, a cerebral angiogram is required to see the carotid encasement. Dynamic MR imaging relies upon the altered contrast enhancement of pituitary microadenomas in relation to the normal gland. Tumours usually enhance at a later time point compared to the normal gland. This timing correlates with tumour size, vascularity, integrity of the blood–brain barrier, and also physical consistency (Kanou et al. 2002). Inferior petrosal sinus sampling (IPSS) is a useful test in determining the site of ACTH overproduction in Cushing's disease (Deipolyi et al. 2011).

Pituitary tumours are graded as microadenoma (diameter less than 1 cm) and macroadenoma (diameter more than 1 cm). Some pituitary adenomas that do not breach the sellar floor are classified as non-invasive and those that breach it are invasive adenomas (Table 2) (Hardy and Vezina 1976).

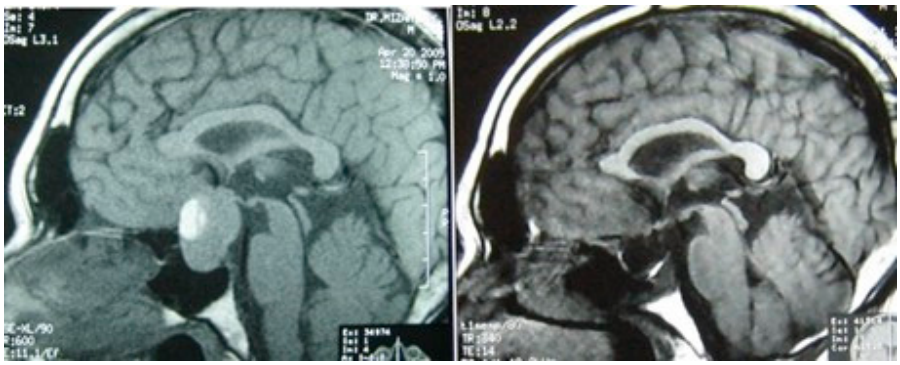

Figure 20. Non-functioning macroadenomas usually present with visual symptoms due to their suprasellar extension. MRI of brain sagittal sections in TW1. (**left**) preoperative image showing pituitary macroadenoma; (**right**) postoperative image showing excision of tumour. Source: Figure by authors.

Table 2. Description of the Hardy and Vezina classification.

Grade/Type	Description
Hardy classification grade	
Sellar invasion	
Grade 0	The enclosed adenoma is described as a tumour that remains within the anatomical confines of the osteoaponeural sheath of the sella turcica. The floor of the sella is always intact.
Grade 1	The sella turcica is within normal limits in size (less than 16 × 13 mm; 208 mm^2) but shows a lowering of the floor on one side or a bulging of the cortex.
Grade 2	The sella turcica is enlarged to various degrees but the floor remains intact.
Grade 3	The sella is more or less enlarged but there is a local erosion or destruction of the floor.
Grade 4	The entire floor of the sella is diffusely eroded or destroyed, producing a characteristic "phantom sella" with all the boundaries barely visible.
Suprasellar extension	
Type A	The suprasellar expansion bulges into the chiasmatic cistern but does not reach the floor of the anterior third ventricle.
Type B	The tumour reaches the floor of the third ventricle, producing the image of an inverse cupula of the anterior recesses of the third ventricle.
Type C	A voluminous suprasellar expansion bulges largely into the third ventricle up to the foramen of Monro.
Type D	Rare aberrant expansions occur in temporal or frontal fossa.

Source: Authors' compilation based on data from Hardy and Vezina (1976).

One of the most often used methods to assess the risk of pituitary macroadenomas invading the cavernous sinus is the Knosp classification. The Knosp classification primarily assesses the extent of the tumour extending across into the cavernous sinus, with a focus on its relation to the cavernous carotid (Knosp et al. 1993).

Predicting residual tumour after resection and operational planning benefit from the Knosp classification, which stratifies the probability of cavernous sinus invasion. Following resection, low Knosp grades are linked to a noticeably higher likelihood of surgical remission.

Knosp Classification

Three lines (Knosp et al. 1993) are drawn between the supraclinoid internal carotid artery and intracavernous internal carotid artery on coronal MR images (Figure 21).

1. Medial tangent;
2. Intercarotid line;
3. Lateral tangent.

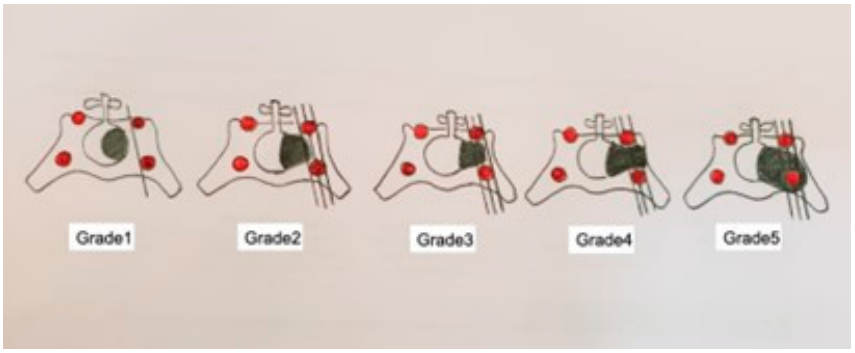

Figure 21. Schematic presentation of Knosp grading of pituitary tumours. Source: Figure by authors; courtesy of Dr. Hafiz Asif Raihan, Neurosurgeon, National Institute of Neurosciences and hospital, Dhaka.

These lines are used to define four grades of tumour invasion:

Grade 0: tumour remains medial to the medial tangent;
Grade 1: tumour extends to between the medial tangent and the intercarotid line;
Grade 2: tumour extends to between the intercarotid line and the lateral tangent;
Grade 3: tumour extends lateral to the lateral tangent;
Grade 3A: tumour extends above the intracavernous internal carotid artery into the superior cavernous sinus compartment.

5.1.3. Treatment Considerations

The principal management of pituitary tumours is both medical and surgical. The only pituitary tumour for which medicinal therapy is the major mode of treatment is prolactinoma. The usual drugs are bromocriptine, cabergoline, and pergolide. Indications for the surgical resection of prolactinoma include drug resistance and intolerance, prolactinoma with cerebrospinal fluid (CSF) leak, acute onset of severe visual or neurological symptoms, or pituitary tumour apoplexy. For acromegaly patients, there are some options for medical treatment with dopamine agonists, somatostatin analogues, and GH antagonists.

The surgical approach could be trans-sphenoidal or transcranial.

The trans-sphenoidal approach could be sublabial or endonasal. Endonasal endoscopy is a versatile approach to deal with pituitary tumours. In endoscopy, there is no external scar and no brain retraction; it is an extra-arachnoid approach and provides a direct landing to the tumour. However, a few complications, like electrolyte imbalance or CSF leak, may occur with this approach.

The transcranial approach still plays an important role in giant and complex pituitary adenomas with wide intracranial extension, brain parenchymal involvement, and the encasement of neurovascular structures. Conventional indications for transcranial approaches include the following:

- Absent pneumatization of the sphenoid sinus;
- Ectatic/kissing internal carotid arteries;

- Reduced dimensions of the sella;
- Lateral involvement of the cavernous sinus lateral to the internal carotid artery;
- Dumbbell-shaped tumours caused by sharp diaphragmatic constriction;
- Calcified/fibrous tumour consistency;
- Wide supra-, para-, and retrosellar extension;
- Arterial encasement;
- Brain invasion;
- Co-existing cerebral aneurysms;
- Separate coexisting pathologies of the sphenoid sinus, especially infections.

Residual/recurrent tumours and postoperative pituitary apoplexy after trans-sphenoidal surgery require individualized considerations (Luzzi et al. 2023).

Radiotherapy is mainly used as an adjuvant therapy to reduce tumour growth in the postsurgical residuum when it cannot be removed safely. Chemotherapy is rarely used in pituitary tumours, except as a salvage treatment for very aggressive pituitary adenomas where other treatment modalities have been exhausted. Oral temozolamide has been used in this regard, with favourable response (Syro et al. 2011).

Acromegaly

Acromegaly is a rare condition brought on by an overabundance of growth hormone (GH), usually as a result of an anterior pituitary adenoma. Insulin-like growth factor 1 (IGF-1) is produced as a result, which leads to the typical proliferation of some tissues. This causes the hands and feet to enlarge, the facial features to coarsen, and it also affects several bodily systems. Acromegaly has three main causes: excess growth hormone-releasing hormone (GHRH), ectopic or iatrogenic GH excess, and primary GH excess (Adigun et al. 2023).

A somatotroph GH-secreting adenoma of the anterior pituitary gland is the most common cause of acromegaly. Additionally, GH excess can be ectopic and generated by cancers other than pancreatic islet cell tumours and lymphomas. Excessive GH administration can potentially lead to iatrogenic GH overload. More rarely, the causes of acromegaly are associated with high GHRH. These can be separated into two categories: core and peripheral causes. Choristomas, ganglioneuromas, and hypothalamic hamartomas are examples of central causes. Adrenal adenoma, small-cell lung carcinoma, and bronchial carcinoid tumours are examples of peripheral causes that release GHRH (Adigun et al. 2023).

The clinical features of acromegaly include joint pain, wrist pain, snoring and sleep apnoea, headaches and visual disturbances, erectile dysfunction or low sex drive, abnormal menses in women, sweaty palms and soles (hyperhidrosis), deepening of the voice, coarse facial features, prominent forehead, prominent brow, prognathism (mandibular enlargement), prominent forehead crease and nasolabial folds, macroglossia and widely spaced dentition, thick eyelids, large nose, acral enlargement (i.e., large hands (with stubby fingers) and feet), proximal myopathy, carpal tunnel syndrome, acromegalic cardiomyopathy, dorsal kyphosis, systemic hypertension, and diabetes mellitus (Adigun et al. 2023).

Serum IGF-1 is employed because, unlike serum GH, it is not affected by changes in sleep patterns, levels of exercise, or the time of day. Elevated IGF-1 levels validate GH excess, and the next step should be imaging to pinpoint the cause. A pituitary MRI is the preferred imaging modality. A CT scan is useful in operative planning. Control of diabetes and hypertension, perioperative airway management, and paying attention to myopathy and cardiomyopathy are very important (Adigun et al. 2023).

Surgery (trans-sphenoidal/transcranial) is the treatment of choice for all microadenomas and macroadenomas. Patients who do not want surgery, are too high risk for surgery, are not candidates for surgery because the tumour might not be resectable, and who have recurrent disease after initial surgical care but are not eligible for repeat surgery are taken into consideration for this. As previously mentioned, neoadjuvant medication therapy may potentially be beneficial prior to surgery. Somatostatin analogues (octreotide, Lanreotide, pasireotide) and GH-receptor antagonists (pegvisomant) are used for medical management. When medical therapy fails to control a patient's disease or there is a recurrence after surgery, radiotherapy (conventional/stereotactic) may be explored as a treatment option. It is imperative to properly follow patients receiving radiation therapy for hypopituitarism (Adigun et al. 2023).

Cushing's Disease

Increased anterior pituitary production of adrenocorticotropic hormone (ACTH) causes the adrenal glands to release too much cortisol, which is the hallmark of Cushing's syndrome, an endocrine disorder. This is frequently brought on by an adenoma of the pituitary gland or by the hypothalamus producing too much corticotropin-releasing hormone (CRH). Pituitary adenomas, which are frequently invisible on imaging tests, are almost always present in Cushing's disease patients. Still, even in the absence of ectopic release of corticotropin-releasing hormone (CRH), rare cases may arise from diffuse corticotroph cell hyperplasia. Microadenomas, which are less than 10 mm in size, make up the majority of these tumours; only 5–10% are macroadenomas (Kairys et al. 2023).

Menstrual irregularities, high blood pressure, diabetes mellitus, widespread weakness, and psychological disorders are among the disease's symptoms. Excess cortisol can be physically manifested as a moon face, buffalo hump, abdominal striae, easy bruising, obesity, facial plethora, and hirsutism. Individuals diagnosed with hypercortisolism typically have a 50% increase in body weight, acne, flushing, poor wound healing, lower limb oedema, fatigue, osteoporosis, myopathy, skin hyperpigmentation, mood and memory abnormalities, decreased sexual drive, or recurrent infections (Kairys et al. 2023).

Biochemical testing includes salivary and serum cortisol testing, 24-h urinary free cortisol testing, serum ACTH assay, and a low-dose overnight dexamethasone suppression test. If an ACTH-secreting tumour is present, a pituitary MRI may reveal it. Nonetheless, in 40% of Cushing's disease patients, MRI is unable to identify a tumour. Tumours visible on MRI have an average size of roughly 6 mm. Implicit petrosal sinus sampling is the most reliable diagnostic test for distinguishing between an adrenal or ectopic Cushing's syndrome and a pituitary tumour. This invasive technique quantifies the variation in ACTH levels between the periphery and the inferior petrosal sinus, which is where the pituitary gland drains (Kairys et al. 2023).

In the event that a primary ACTH-secreting tumour is discovered, trans-sphenoidal surgery is the initial line of treatment for the adenoma. Pituitary radiation therapy is an alternative that may be utilized following a failed trans-sphenoidal surgery. Finally, individuals with Cushing's disease may have an instant decrease in cortisol levels with bilateral adrenalectomy, but after that, they will need to take glucocorticoid and mineralocorticoid replacement medication for the rest of their lives. Nelson's syndrome is one of the main side effects of this treatment (Kairys et al. 2023).

5.2. Craniopharyngioma

5.2.1. Clinical Considerations

Craniopharyngioma is a rare tumour which is considered histologically benign but acts in a malignant way because of its close proximity to eloquent brain structures, unexpected biologic behaviour, and high local recurrence rate. It may result in significant endocrine, visual, and neurocognitive morbidity. Across all ages, it constitutes only around 1% of all new CNS tumours found per year, although this rises to 4% in the paediatric group of patients (Dolecek et al. 2012). There is a bimodal age distribution with two peaks, one in middle-to-late adulthood (45–65 years of age) and the other during school age (5–14 years). There is no sex-based preference. While adamantinomatous tumours can be found in both groups, the papillary form of a craniopharyngioma is typically observed in adults.

From an embryological point of view, craniopharyngiomas develop as a result of an improper or incomplete involution of the craniopharyngeal duct and Rathke's pouch, which results in nests of resting epithelial cells that later develop into neoplasms (Prabhu and Brown 2005; Senthilvel et al. 2014). In the mature adult pituitary gland, metaplasia is thought to give rise to papillary tumours.

Craniopharyngiomas and the circle of Willis and its branch are intimately related. The exact anatomical relationship with the optic nerve is very important when planning a surgical approach (Steno et al. 2004), whether normal (above the midpoint of the sella), prefixed (above the tuberculum sella), or postfixed (above the dorsum sella). It can be infradiaphragmatic or supradiaphragmatic (suprasellar extraventricular, intraventricular extraventricular, or purely intraventricular). Intraventricular extraventricular craniopharyngiomas are the most commonly encountered configuration (Steno et al. 2004). These are WHO grade 1 tumours.

According to gross pathologic examination, craniopharyngiomas can be categorized as cystic (50%), mixed cysto-solid (35%), and solid (15%). Secondary changes like fibrosis, calcification, ossification, and cholesterol

deposits may occur (Fernandez-Miranda et al. 2012). Cysts are noted to have a brownish-coloured fluid often described as resembling machine oil. Calcification is frequently identified in these tumours.

The symptoms of a craniopharyngioma can be diverse due to the involvement of very important surrounding neurovascular structures. They can be visual (due to injury to or compression of the optic apparatus), endocrine (hypothalamic–pituitary axis), neurocognitive (hypothalamus, mammillary bodies, and associated limbic structures), and of obstructive hydrocephalus. Hydrocephalus and endocrinopathies are commoner in paediatric patients, and impaired vision and neurocognitive changes are commoner in adult patients.

Visual impairment can either be reduced acuity or visual field defects. The different patterns of field defects include bitemporal hemianopia, concentric field defect, homonymous hemianopia, and paracentral or central scotoma. Fundal examination may reveal papilloedema with hydrocephalus or optic atrophy with direct chasmal compression. Children may have stunted development or delayed puberty. Adults may experience amenorrhoea in women or a diminished libido in men due to erectile dysfunction. A thorough neuro-ophthalmologic and endocrine evaluation of the anterior and posterior pituitary gland is necessary at presentation. Obesity and diabetes insipidus resulting from antidiuretic hormone deficiency can also occur with these tumours. Children may have decreased school performance and have the classical triad of hypothyroidism, hypogonadism, and growth retardation (Fernandez-Miranda et al. 2012).

5.2.2. Investigative Considerations

Endocrinopathies can be fatal and significantly reduce a patient's quality of life. Growth hormone is the most often affected hormone in people with hypopituitarism, with 85% of patients affected presentation (Van Effenterre and Boch 2002). A plain X-ray of the skull reveals patchy or rim calcification, erosion of the dorsum sellae, a copper beaten appearance of the skull, and sutural diastasis due to raised intracranial pressure. A CT scan is useful to delineate tumour morphology, hydrocephalus, and calcification.

Craniopharyngiomas are usually lobulated, cystic suprasellar masses. Cyst contents may have increased density compared to the CSF. Calcification is around 85% to 90% in childhood and around 40% to 50% in adult tumours. One of the typical features is eggshell calcification. MRI of the brain gives a detailed view of the tumour, including compression of the optic nerve and of vascular structures, especially the internal carotid artery, and its relationship with delicate neural structures. On MRI, these tumours are usually heterogenous (Figure 22). Sometimes, an angiogram is required to see the vascular relationship before surgical exploration (Fernandez-Miranda et al. 2012).

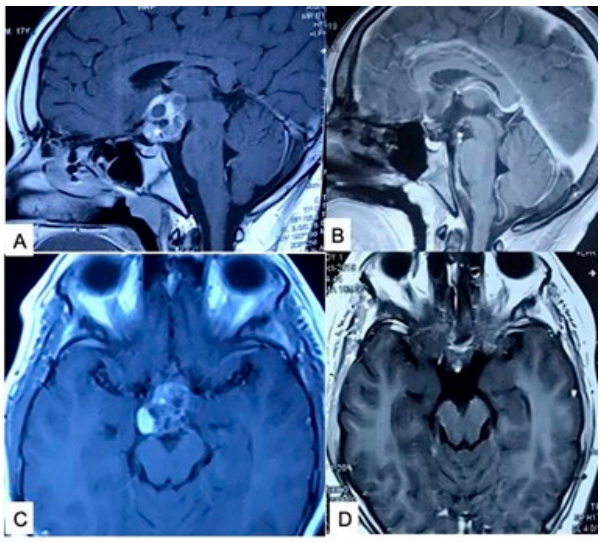

Figure 22. Contrast MRI of brain. (**A**,**C**) Preoperative craniopharyngiomas typically have both solid and cystic components, associated with calcifications. (**B**,**D**) Postoperative contrast MRI showing a very small portion of residual tumour adherent to the pituitary stalk. Source: Figure by authors.

5.2.3. Treatment Considerations

Before definitive surgical treatment, it is important to correct the endocrine and biochemical abnormalities. There are different surgical approaches, like transcranial and trans-sphenoidal. The surgical approach will differ

based on the site and area of involvement of the tumour. An essential factor in choosing an approach is the stalk and optic chiasm's location with respect to the sella. The location of the chiasm can vary: it might be postfixed above the dorsum sellae, above the diaphragm or the middle of the sellae (normal), or above the tuberculum (prefixed) (Rhoton 2002). Subfrontal and/or trans-sylvian approaches can be employed to deal with these tumours in different craniotomies, like pterional, frontotemporal, or frontotemporal–orbito-zygomatic. The surgical corridors can be interoptic, optico-carotid, carotico-sylvian, or trans-lamina terminalis. The edonasal endoscopic trans-sphenoidal approach is a very good option to deal with infradiaphragmatic tumours. Sometimes, in cystic tumours, endoscopic cyst aspiration with the placement of an Ommaya reservoir can be used in order to aspirate the cyst from time to time in case of raised ICP. Intralesional bleomycin can also be given through this reservoir. Other treatment modalities include conventional radiotherapy, proton beam therapy, and stereotactic radiosurgery (SRS) (Fernandez-Miranda et al. 2012).

The prognosis of these tumours depends upon the maximal safe surgical resection and on the regular endocrine and biochemical assessment of the patients. Because of the critical anatomical location, no tumour should be forcibly pulled away from the optic nerve, vessels, or hypothalamus, and accepting a subtotal resection is often the safest option.

5.3. Rathke's Cleft Cyst

5.3.1. Clinical Considerations

Rathke's pouch is the region where the anterior and posterior pituitary glands converge. Normally, this pouch closes quite early in embryonic development. When a remnant enlarges into a cleft, it is known as Rathke's cleft cyst. It is a primary brain tumour that is extremely uncommon and often affects adults. Typically, it is a non-neoplastic lesion that is predominantly intrasellar and rarely suprasellar. A single layer of cuboidal epithelium lines it. This tumour may present as visual impairment and hypopituitarism. It can be asymptomatic or may present with headache and/or variable presentation due to compression of the hypothalamus, pituitary stack, pituitary gland, and optic chiasma (Naik and Thakore 2013).

5.3.2. Investigative Considerations

Thorough neuro-ophthalmic and endocrine evaluation is required. Both CT scan and MRI scan can reveal the cystic lesion. CT scans depict a discrete low-density intrasellar lesion which usually does not calcify. MRI reveals increased intensity on T1 WI in two-thirds of cases; this is variable on T2 WI. This lesion usually does not enhance on contrast but an enhancing rim may sometimes be seen (Naik and Thakore 2013).

5.3.3. Treatment Considerations

The cystic fluid may resemble motor oil. Surgery for this cystic lesion includes draining the fluid from the cyst. Most neurosurgeons now prefer the minimally invasive endoscopic approach, which minimizes complications, hospitalization time, and discomfort.

6. Pineal Tumours

6.1. Clinical Considerations

The pineal region is surrounded by the tentorial apex from the back, by the culmen of the cerebellar vermis from below, by the splenium of the corpus callosum from above, and by the third ventricle, quadrigeminal plate, and midbrain tectum from the front. The great cerebral vein of Galen, which is created by the union of the internal cerebral veins above the pineal gland and the basal vein of Rosenthal that emerges laterally from the ambient cisterns, is one of a number of crucially significant venous systems that converge in the pineal area.

The pineal area is prone to both neoplastic and non-neoplastic tumour development. Pineal tumours, 60% of which are germ cell tumours, comprise germinoma, mature teratoma, and immature teratoma with malignant transformation; they also include embryonal carcinoma, yolk sac tumours, and choriocarcinoma. Pineocytoma, pineal parenchymal neoplasms of intermediate differentiation, pineoblastoma, and papillary tumours of the pineal area are tumours originating from glandular tissue. Astrocytoma, ependymoma, glioma, choroid plexus papilloma, meningioma, haemangioma, chemodectoma, and metastases are examples of other tumours (Al-Hussaini et al. 2009). Arachnoid cysts, cysticercoses, arteriovenous malformations, cavernomas, and vein of Galen malformations

are non-neoplastic abnormalities of this area. Tumours of the pineal region affect children more frequently than adults. While meningioma and glioma predominate in adults, germinoma or astrocytoma are the commonest tumour types in children.

The symptoms of raised intracranial pressure, cerebellar signs, hydrocephalus, and local compression of the dorsal midbrain are those most frequently associated with pineal region tumours (Konovalov and Pitskhelauri 2003). The typical symptoms of these tumours include headache, nausea, Parinaud syndrome, and double vision. Compression of the posterior commissure and of the rostral interstitial nucleus of the medial longitudinal fasciculus results in Parinaud syndrome (dorsal midbrain syndrome). Upgaze paralysis, convergence–retraction nystagmus induced by a quick upward gaze, pseudo-Argyll Robertson pupils, retraction of the eyelids (Collier's sign), and, occasionally, a conjugate downward look at baseline (i.e., setting sun sign) are the symptoms of this syndrome. The patient may also exhibit extrapyramidal movement disorder, precocious puberty, hypothalamic dysfunction, DI, thalamic pain, and endocrine instability. Pineal cell tumours, ependymoma, and germ cell tumours metastasize quickly in the CSF (drop metastasis).

6.2. Investigative Considerations

For germ cell tumours, tumour markers can occasionally be employed as diagnostic as well as prognostic tools. Increased levels of AFP are often linked to yolk sac tumours, but high levels of β-HCG are classically linked to choriocarcinoma (moderate rise in germinoma and embryonal carcinoma; mild elevation in teratoma and embryonal carcinoma). A higher level of placental alkaline phosphatase is also observed in germinoma, yolk sac tumours, and choriocarcinoma. A worse prognosis is linked to higher serum tumour marker levels.

For diagnosis, CT scan and MRI (Figure 23a,b) can delineate the tumour details, hydrocephalus, and compression of surrounding structures. To evaluate drop metastasis, MRI of the cervical, thoracic, and lumbar spine is occasionally performed. The major purpose of tumour markers is to determine the prognosis.

Pure germinomas comprise 55–65% of all intracranial germ cell tumours and are identified synchronously in both the pineal gland and in the suprasellar region in 10% of cases (Matula 2012; Raiyawa et al. 2012). Here, alpha-fetoprotein (AFP) in the CSF as a tumour marker, lumbar puncture, and stereotactic biopsy can be used as diagnostic tools, and radio-chemotherapy is used as the standard of care, as these lesions are very sensitive to both radiation and chemotherapy.

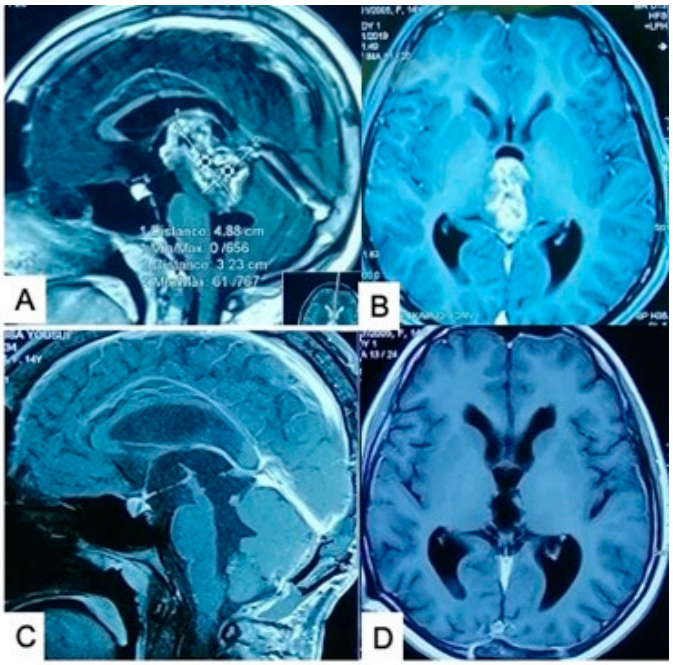

(**a**)

Figure 23. *Cont.*

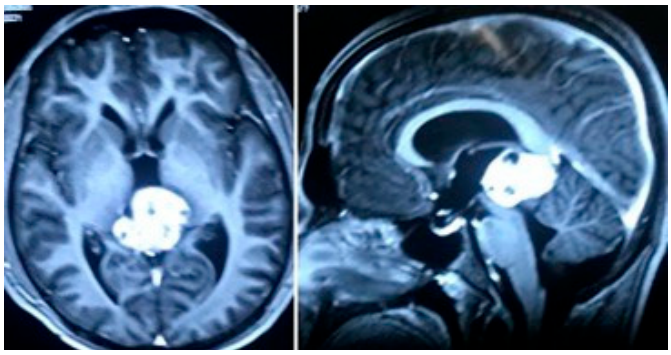

(**b**)

Figure 23. (**a**) Contrast MRI of brain showing preoperative (**A**,**B**) and postoperative (**C**,**D**) images of pineal and posterior 3rd ventricular grade 2 ependymoma. (**b**) Contrast MRI of brain; axial and sagittal view showing pineal immature teratoma in a 15-year-old boy. Source: Figure by authors.

6.3. Treatment Considerations

The most emergency triage or urgent approach is to place an external ventricular drainage. The standard approach in some institutions is a simultaneous endoscopic pineal tumour biopsy and an endoscopic third ventriculostomy, particularly for radio- and chemosensitive tumours like germinoma. Alternatively, some neurosurgeons insert a preoperative ventriculoperitoneal shunt first and plan for a definitive surgery once the acute condition is resolved. Some surgeons insert a shunt between the third ventricle and the cisterna magna after tumour excision (Figure 24).

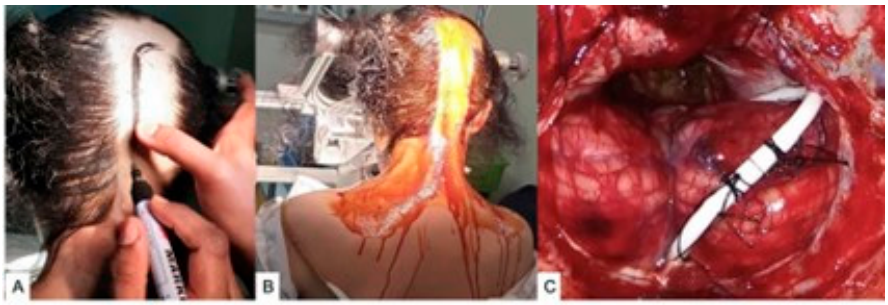

Figure 24. Intraoperative pictures: (**A**,**B**) Sitting position and incision mark for supracerebellar infratentorial approach to pineal tumour. (**C**) Intraoperative insertion of 3rd ventriculo-cisternal (cisterna magna) shunt after tumour removal. Source: Figure by authors.

In 1931, Oppenheim and Krause became the pioneers in the surgical removal of a pineal region tumour via a supracerebellar infratentorial approach (Oppenheim and Krause 1913). Dandy reported the first GTR with the interhemispheric transcallosal approach. Van Wagenen (Van Wagenen 1931) described a transcortical transventricular approach in 1931. Poppen described the occipital transtentorial approach. The anterior transchoroidal approach is preferred when the pineal tumour has spread into the anterior third ventricle.

7. Intraventricular Tumours

7.1. Clinical Considerations

According to the US Central Brain Tumour Registry, about 1.2% of primary brain tumours are intraventricular in location. They represent a diverse group of tumours of variable histopathology, but most are low-grade tumours. They can be confined to one ventricle or can extend into an adjacent ventricle or into an adjacent cistern through the outflow foramina. Large tumours can extend into the parenchyma through the ependymal wall (Ostrom et al. 2013; Louis et al. 2016).

Some of the most common tumours arising from the lateral ventricles are ependymomas, subependymal giant-cell astrocytomas, subependymomas, central neurocytomas, astrocytomas, meningiomas, lymphomas, and choroid plexus tumours. Among third ventricular tumours, colloid cysts, choroid plexus papillomas and carcinomas, meningiomas, craniopharyngiomas, and germ cell tumours are common. Ependymomas and subependymomas

are fourth ventricular tumours. Medulloblastomas are usually vermian tumours but frequently present as large tumours within the cerebellar hemispheres. Large, intraparenchymal, high-grade astrocytic tumours can become exophytic into the lateral ventricles and may obliterate the foramen of Monro or cut off the posterior lateral ventricle and cause obstructive hydrocephalus.

Central neurocytomas originate from precursors of neuronal cells that exist within the septum pellucidum. They have a wide attachment on the septum pellucidum and can grow to a significant size within the lateral ventricles and third ventricle through the foramen of Monro. They are well circumscribed, can be lobulated, contain cysts and heterogenous signal and flow voids, and can contain calcification.

Subependymomas are well-circumscribed non-enhancing benign tumours most frequently seen in the ventricle. Surgical resection is indicated if they become symptomatic or progressive on imaging. Subependymal giant-cell astrocytomas are tumours of mixed and neuronal differentiation arising from subependymal nodules and are common in patients with tuberous sclerosis. Ependymomas in adults are more frequent in the fourth ventricle but they can also be seen within the lateral ventricles. They are also the most common intramedullary spinal cord tumours. They are well-circumscribed tumours that enhance and frequently contain calcifications.

Meningiomas are the commonest intraventricular tumours in the trigone of the lateral ventricle. They presumably originate from arachnoid cap cells trapped within the choroid plexus during embryonal life. They may reach a large size and cause symptoms suggestive of high intracranial pressure, but they can be also incidental. Treatment options include surgery, SRS, and surveillance.

Choroid plexus tumours arise from the choroid plexus and are most commonly located in the lateral ventricle in children and the fourth ventricle in adults. Histologically, they can be choroid plexus papillomas (WHO grade 1), atypical choroid plexus papillomas (WHO grade 2), and choroid plexus carcinomas (WHO grade 3). They tend to present with hydrocephalus both due to increased CSF production and due to obstruction.

Colloid cysts are the commonest third ventricular tumours. They are benign lesions consisting of epithelial-lined cysts filled with gel-density material which contains mucin, cholesterol, and hyaloid substances. They can be diagnosed as an incidental finding or present with acute, intermittent, or chronic obstructive hydrocephalus. Sudden death is rare but has been reported. Surgical options include open surgery via a transcortical or transcallosal approach, endoscopic excision, or frameless stereotactic aspiration.

The extension of a sellar mass into the third ventricle may produce visual field disturbances and hormone disturbances on endocrine profile. Suprasellar tumours extending into the ventricles include craniopharyngioma, germinoma, meningioma, and optic pathway and hypothalamic glioma. Common posterior third ventricular tumours include pineal region tumours, meningiomas, arachnoid cysts, and dermoid cysts.

Medulloblastomas originate from the cerebellar vermis and most commonly occur in the paediatric population. They usually present with acute hydrocephalus. The 2016 WHO CNS tumour classification provides a very useful presentation of the usual combinations of the well-established histological subtypes of these tumours (desmoplastic/nodular, medulloblastoma with extensive nodularity, large-cell, and anaplastic) and of the four currently established genetic subtypes (WNT-activated, SHH-activated, group 3 subtype, and group 4 subtype). At the time of presentation, a significant percentage of patients already have secondary deposits in the spine.

The presentation of intraventricular tumours depends on their location, size, and progression rate. Rapid progression can cause acute hydrocephalus that requires CSF diversion before the definite management of the tumour. Slow-growing tumours are asymptomatic for a long time before they become symptomatic and usually present with a chronic, NPH-like clinical picture. Apart from diagnostic imaging, preoperative imaging of the whole craniospinal axis and CSF sampling are indicated for tumours with known potential for CSF dissemination. Head CT and MRI of the head with contrast are needed for diagnosis, evaluation of anatomical details, and surgical planning (Figure 25) (Ostrom et al. 2013; Louis et al. 2016).

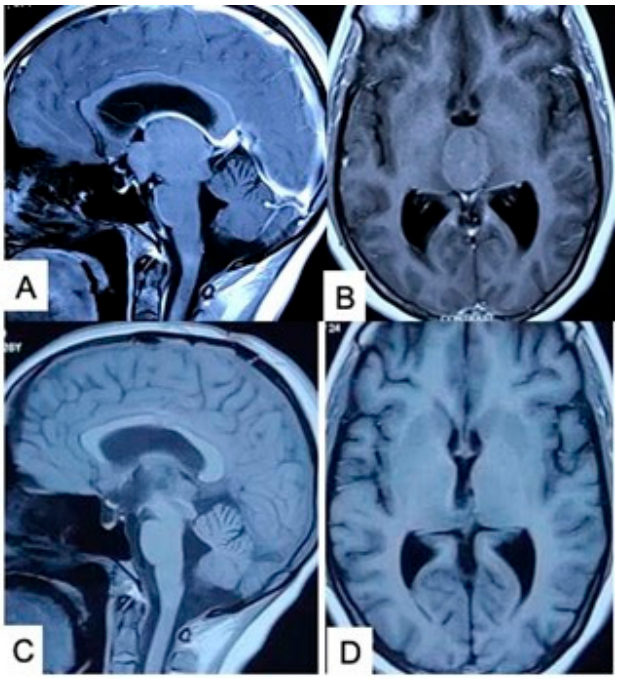

Figure 25. MRI of brain. (**A**,**B**) T1-weighted contrast-enhanced preoperative images showing non-contrast-enhancing 3rd ventricular grade 1 glioma. (**C**,**D**) Postoperative images showing removal of tumour via interhemispheric transcallosal transchoroidal approach. Source: Figure by authors.

7.2. Treatment Considerations

The management of hydrocephalus is the first consideration. For third ventricular tumours, neuro-endoscopy can obtain both CSF diversion (ETV+/- septostomy) and a biopsy. CSF diversion should be carried out first as the biopsy can cause bleeding from the tumour, causing reduced visibility. Conservative management with serial imaging follow-up may be the best option if the patient is asymptomatic, the tumour is not growing, or the patient is not fit for surgery. For older and unfit patients and when the tumour is considered low-grade with an indolent clinical course, CSF diversion alone may be the best alternative. The surgical approach for tumour resection depends on the specific site and extension of the tumour (Ostrom et al. 2013; Louis et al. 2016).

Author Contributions: Conceptualization, methodology, validation, formal analysis, investigation, resources, data curation, M.R.H., R.A.K. and S.I.M.K.N.K.; writing—original draft preparation, M.R.H. and R.A.K.; writing—review and editing, visualization, supervision, F.H.C. All authors have read and agreed to the published version of the manuscript.

Funding: This research received no external funding.

Conflicts of Interest: The authors declare no conflicts of interest.

References

Adigun, Oluwaseun O., Minhthao Nguyen, Tamaryn J. Fox, and Catherine Anastasopoulou. 2023. Acromegaly. In *StatPearls [Internet]*; Treasure Island: StatPearls Publishing. Available online: https://www.ncbi.nlm.nih.gov/books/NBK431086/ (accessed on 2 February 2023).

Akar, Ziya, Necmettin Tanriover, Saffet Tuzgen, Ali M. Kafadar, and Cengiz Kuday. 2003. Surgical treatment of intracranial epidermoid tumors. *Neurologia Medico-Chirurgica* 43: 275–80. [CrossRef] [PubMed]

Alalade, Andrew Folusho, and Neil D. Kitchen. 2018. Convexity and Parasagittal Versus Skull Base Meningiomas. In *Principles of Neurological Surgery*. Edited by R. G. Ellenbogen, L. N. Shekhar and N. D. Kitchen. Philadelphia: Elsevier, pp. 593–601.

Albert, Friedrich K., Michael Forsting, Klaus Sartor, Hans-Peter Adams, and Stefan Kunze. 1994. Early postoperative magnetic resonance imaging after resection of malignant glioma: Objective evaluation of residual tumor and its influence on regrowth and prognosis. *Neurosurgery* 34: 45–60. [CrossRef] [PubMed]

Al-Hussaini, Maysa, Iyad Sultan, Najyah Abuirmileh, Imad Jaradat, and Ibrahim Qaddoumi. 2009. Pineal gland tumours: Experience from the SEER database. *Journal of Neuro-Oncology* 94: 351–58. [CrossRef] [PubMed]

Al-Mefty, Ossama. 1991. Clinoidal meningiomas. In *Meningiomas*. Edited by Ossama Al-Mefty. New York: Raven Press, pp. 427–43.

Al-Mefty, Ossama, John L. Fox, and Robert R. Smith. 1988. Petrosal approach for petroclival meningiomas. *Neurosurgery* 22: 510–17. [CrossRef]

Almefty, R., G. F. Haddad, and O. Al-Mefty. 2017. Meningiomas. In *Youmans & Winn Neurological Surgery*. Edited by H. R. Winn. Philadelphia: Elsevier, pp. 1107–33.

Ang, Celina, David Hauerstock, Marie-Christine Guiot, Goulnar Kasymjanova, David Roberge, Petr Kavan, and Thierry Muanza. 2008. Characteristics and outcomes of medulloblastoma in adults. *Pediatric Blood & Cancer* 51: 603–607. [CrossRef]

Asari, Shoji, Tomohide Maeshiro, Susumu Tomita, Masamitsu Kawauchi, Nobuyoshi Yabuno, Kazushi Kinugasa, and Takashi Ohmoto. 1995. Meningiomas arising from the falcotentorial junction: Clinical features, neuroimaging studies, and surgical treatment. *Journal of Neurosurgery* 82: 726–38. [CrossRef]

Belykh, Evgenii, Kurt V. Shaffer, Chaoqun Lin, Vadim A. Byvaltsev, Mark C. Preul, and Lukui Chen. 2020. Blood-Brain Barrier, Blood-Brain Tumor Barrier, and Fluorescence- Guided Neurosurgical Oncology: Delivering Optical Labels to Brain Tumors. *Frontiers in Oncology* 10: 739. [CrossRef]

Bikmaz, Kerem, Robert Mrak, and Ossama Al-Mefty. 2007. Management of bone-invasive, hyperostotic sphenoid wing meningiomas. *Journal of Neurosurgery* 107: 905–12. [CrossRef]

Birk, Harjus S., Seunggu J. Han, Ramez W. Kirollos, Thomas Santarius, and Michael W. McDermott. 2019. Meningiomas and haemangiopericytoma (HPC). In *Oxford Textbook of Neurological Surgery*. Edited by Ramez Kirollos, Adel Helmy, Simon Thomson and Peter Hutchinson. Oxford: Oxford University Press, pp. 175–89.

Bondy, Melissa L., Michael E. Scheurer, Beatrice Malmer, Jill S. Barnholtz-Sloan, Faith G. Davis, Dora Il'yasova, Carol Kruchko, Bridget J. McCarthy, Preetha Rajaraman, Judith A. Schwartzbaum, and et al. 2008. Brain tumor epidemiology: Consensus from the Brain Tumor Epidemiology Consortium. *Cancer* 113: 1953–68. [CrossRef]

Brown, Timothy J., Matthew C. Brennan, Michael Li, Ephraim W. Church, Nicholas J. Brandmeir, Kevin L. Rakszawski, Akshal S. Patel, Elias B. Rizk, Dima Suki, Raymond Sawaya, and et al. 2016. Association of the extent of resection with survival in glioblastoma: A systematic review and meta-analysis. *JAMA Oncology* 2: 1460–69. [CrossRef]

Castillo, Mauricio, J. Keith Smith, and Lester Kwock. 2000. Correlation of myo-inositollevels and grading of cerebral astrocytomas. *AJNR American Journal of Neuroradiology* 21: 1645–49. [PubMed]

Chandler, C. 2019. Ependymoma. In *Oxford Textbook of Neurological Surgery*. Edited by Ramez Kirollos, Adel Helmy, Simon Thomson and Peter Hutchinson. Oxford: Oxford University Press, pp. 361–66.

Chang, Steven D., and Gordon T. Sakamoto. 2003. The role of radiosurgery for hemangioperi- cytomas. *Neurosurgical Focus* 14: e14. [CrossRef] [PubMed]

Chiechi, Maria V., James G. Smirniotopoulos, and Hernando Mena. 1996. Intracranial hemangiopericytomas: MR and CT features. *AJNR American Journal of Neuroradiology* 17: 1365–71. [PubMed]

Chowdhury, Forhad, Mohammod Haque, and Mainul Sarker. 2013. Intracranial epidermoid tumor; microneurosurgical management: An experience of 23 cases. *Asian Journal of Neurosurgery* 8: 21–28. [CrossRef]

Cimmino, Flora, Maria Nunzia Scoppettuolo, Marianeve Carotenuto, Pasqualino De Antonellis, Valeria Di Dato, Gennaro De Vita, and Massimo Zollo. 2011. Norcantharidin impairs medulloblastoma growth by inhibition of Wnt/catenin signaling. *Journal of Neuro-Oncology* 106: 59–70. [CrossRef]

Cushing, Harvey, and Louise Eisenhardt. 1938. *Meningiomas: Their Classification, Regional Behaviour, Life History, and Surgical End Results*. Springfield: Charles C Thomas.

Cusimano, Michael D., and Michael Patrick Meier. 2019. Surgical management of anterolateral skull base lesions. In *Oxford Textbook of Neurological Surgery*. Edited by Ramez Kirollos, Adel Helmy, Simon Thomson and Peter Hutchinson. Oxford: Oxford University Press, pp. 241–51.

Damodaran, Omprakash, Peter Robbins, Neville Knuckey, Michael Bynevelt, George Wong, and Gabriel Lee. 2014. Primary intracranial haemangiopericytoma: Comparison of survival outcomes and metastatic potential in WHO grade II and III variants. *Journal of Clinical Neuroscience* 21: 1310–14. [CrossRef]

De Witt Hamer, Philip C., Santiago Gil Robles, Aeilko H. Zwinderman, Hugues Duffau, and Mitchel S. Berger. 2012. Impact of intraoperative stimulation brain mapping on glioma surgery outcome: A meta-analysis. *Journal of Clinical Oncology* 30: 2559–65. [CrossRef]

Deipolyi, Amy, Ali Karaosmanoğlu, Cicero Habito, Scott Brannan, Stephan Wicky, Joshua Hirsch, and Rahmi Oklu. 2011. The role of bilateral inferior petrosal sinus sampling in the diagnostic evaluation of Cushing disease. *Diagnostic and Interventional Radiology* 18: 132–38. [CrossRef]

Dolecek, Therese A., Jennifer M. Propp, Nancy E. Stroup, and Carol Kruchko. 2012. CBTRUS Statistical report: Primary Brain and Central Nervous System Tumors Diagnosed in the United States in 2005–2009. *Neuro-Oncology* 14: v1–v49. [CrossRef]

Duffau, Hugues, Peggy Gatignol, Emmanuel Mandonnet, Laurent Capelle, and Luc Taillandier. 2008. Intraoperative subcortical stimulation mapping of language pathways in a consecutive series of 115 patients with grade II glioma in the left dominant hemisphere. *Journal of Neurosurgery* 109: 461–71. [CrossRef]

Erkmen, Kadir, Svetlana Pravdenkova, and Ossama Al-Mefty. 2005. Surgical management of petroclival meningiomas: Factors determining the choice of approach. *Neurosurgical Focus* 19: E7. [CrossRef] [PubMed]

Fernandez-Miranda, Juan C., Paul A. Gardner, Carl H. Snyderman, Kenneth O. Devaney, Primož Strojan, Carlos Suárez, Eric M. Genden, Alessandra Rinaldo, and Alfio Ferlito. 2012. Craniopharyngioma: A pathologic, clinical, and surgical review. *Head & Neck* 34: 1036–44. [CrossRef]

Fletcher, C., K. K. Unni, and F. Mertens. 2013. *World Health Organization Classification of Tumours of Soft Tissue and Bone*, 4th ed. Geneva: WHO.

Fruehwald-Pallamar, Julia, Stefan B. Puchner, Andrea Rossi, Maria L. Garre, Armando Cama, Claus Koelblinger, Anne G. Osborn, and Majda M. Thurnher. 2011. Magnetic resonance imaging spectrum of medulloblastoma. *Neuroradiology* 53: 387–96. [CrossRef] [PubMed]

Gaspar, Laurie, Charles Scott, Marvin Rotman, Sucha Asbell, Theodore Phillips, Todd Wasserman, W. Gillies McKenna, and Roger Byhardt. 1997. Recursive partitioning analysis (RPA) of prognostic factors in three Radiation Therapy Oncology Group (RTOG) brain metastases trials. *International Journal of Radiation Oncology Biology Physics* 37: 745–51. [CrossRef]

Geffen, G., A. Walsh, D. Simpson, and M. Jeeves. 1980. Comparison of the effects of transcortical and transcallosal removal of intraventricular tumours. *Brain* 103: 773–88. [CrossRef] [PubMed]

GLOBOCAN. 2002. *Worldwide Incidence and Mortality of Cancer, 2002 [Computer Program]*. Lyon: IARC.

Gormley, W. B., F. J. Tomecek, N. Qureshi, and G. M. Malik. 1994. Craniocerebral epidermoid and dermoid tumours: A review of 32 cases. *Acta Neurochirurgica* 128: 115–21. [CrossRef] [PubMed]

Gottardo, Nicholas G., Jordan R. Hansford, Jacqueline P. McGlade, Frank Alvaro, David M. Ashley, Simon Bailey, David L. Baker, Franck Bourdeaut, Yoon-Jae Cho, Moira Clay, and et al. 2014. Medulloblastoma Down Under 2013: A report from the third annual meeting of the International Medulloblastoma Working Group. *Acta Neuropathologica* 127: 189–201. [CrossRef]

Greenberg, Mark S. 2010. *Handbook of Neurosurgery*. New York: Thieme.

Gupta, Anshu, and Tanima Dwivedi. 2017. A simplified overview of world health organization classification update of central nervous system tumors 2016. *The Journal of Neurosciences in Rural Practice* 8: 629–41. [CrossRef]

Guthrie, Barton L., Michael J. Ebersold, Bernd W. Scheithauer, and Edward G. Shaw. 1989. Meningeal hemangiopericytoma: Histopathological features, treatment, and long-term follow-up of 44 cases. *Neurosurgery* 25: 514–22. [CrossRef]

Guthrie, B. L., S. C. Carabell, and E. R. Laws, Jr. 1991. Radiation therapy for intracranial meningiomas. In *Meningiomas*. Edited by Ossama Al-Mefty. New York: Raven Press, p. 255.

Haines, D. E., and R. G. Frederickson. 1991. The meninges. In *Meningiomas*. Edited by Ossama Al-Mefty. New York: Raven Press, pp. 9–25.

Hakyemez, Bahattin, Umit Aksoy, Harun Yildiz, and Necdet Ergin. 2005. Intracranial epidermoid cysts: Diffusion-weighted, FLAIR and conventional MR findings. *European Journal of Radiology* 54: 214–20. [CrossRef]

Hardy, J., and J. L. Vezina. 1976. Transsphenoidal neurosurgery of intracranial neoplasm. In *Advances in Neurology*. Edited by R. A. Tompson and J. R. Green. New York: Raven Press, pp. 261–75.

Hassaneen, Wael, and Raymond Sawaya. 2017. Epidermoid, Dermoid, and Neurenteric Cysts. In *Youmans & Winn Neurological Surgery*. Edited by H. Richard Winn. Philadelphia: Elsevier, pp. 1186–91.

Jukich, Patti J., Bridget J. McCarthy, Tanya S. Surawicz, Sally Freels, and Faith G. Davis. 2001. Trends in incidence of primary brain tumors in the United States, 1985–1994. *Neuro-Oncology* 3: 141–51. [CrossRef] [PubMed]

Kairys, N., C. Anastasopoulou, and A. Schwell. 2023. Cushing Disease. In *StatPearls [Internet]*; Treasure Island: StatPearls Publishing. Available online: https://www.ncbi.nlm.nih.gov/books/NBK448184/ (accessed on 23 March 2023).

Kanou, Yukari, Kazunori Arita, Kaoru Kurisu, A. Tomohide, and Kohji Iida. 2002. Clinical implications of dynamic MRI for pituitary adenomas: Clinical and histological analysis. *Journal of Clinical Neuroscience* 9: 659–63. [CrossRef] [PubMed]

Keil, Margaret F., and Constantine A. Stratakis. 2008. Pituitary tumours in childhood: An update in their diagnosis, treatment and molecular genetics. *Expert Review of Neurotherapeutics* 8: 563–74. [CrossRef]

Kinjo, Toshihiko, Ossama Al-Mefty, and Imad Kanaan. 1993. Grade zero removal of supratentorial convexity meningiomas. *Neurosurgery* 33: 394–99. [PubMed]

Klein, Martin, Hugues Duffau, and Philip C. De Witt Hamer. 2012. Cognition and resective surgery for diffuse infiltrative glioma: An overview. *Journal of Neuro-Oncology* 108: 309–18. [CrossRef] [PubMed]

Kleiser, Raimund, Philipp Staempfli, Anton Valavanis, Peter Boesiger, and Spyros Kollias. 2010. Impact of fMRI-guided advanced DTI fiber tracking techniques on their clinical applications in patients with brain tumors. *Neuroradiology* 52: 37–46. [CrossRef] [PubMed]

Knosp, Engelbert, Erich Steiner, Klaus Kitz, and Christian Matula. 1993. Pituitary adenomas with invasion of the cavernous sinus space: A magnetic resonance imaging classification compared with surgical findings. *Neurosurgery* 33: 610–17. [CrossRef]

Konovalov, Alexander N., and David I. Pitskhelauri. 2003. Principles of treatment of the pineal region tumours. *Surgical Neurology* 59: 250–68. [CrossRef]

Kool, Marcel, David T. W. Jones, Natalie Jäger, Paul A. Northcott, Trevor J. Pugh, Volker Hovestadt, Rosario M. Piro, L. Adriana Esparza, Shirley L. Markant, Marc Remke, and et al. 2014. Genome sequencing of SHH medulloblastoma predicts genotype-rdated response to smoothened inhibition. *Cancer Cell* 25: 393–405. [CrossRef]

Kowalczuk, Andrew, R. Loch Macdonald, Chris Amidei, George Dohrmann III, Robert K. Erickson, Javad Hekmatpanah, Stuart Krauss, Swarna Krishnasamy, Gregory Masters, Sean F. Mullan, and et al. 1997. Quantitative imaging study of extent of surgical resection and prognosis of malignant astrocytomas. *Neurosurgery* 41: 1028–36. [CrossRef]

Krivosheya, Daria, Sujit S. Prabhu, Jeffrey S. Weinberg, and Raymond Sawaya. 2016. Technical principles in glioma surgery and preoperative considerations. *Journal of Neuro-Oncology* 130: 243–52. [CrossRef] [PubMed]

Kubben, Pieter L., Karlien J. ter Meulen, Olaf EMG Schijns, Mariël P. ter Laak-Poort, Jacobus J. van Overbeeke, and Henk van Santbrink. 2011. Intraoperative MRIguided resection of glioblastoma multiforme: A systematic review. *The Lancet Oncology* 12: 1062–70. [CrossRef] [PubMed]

Kumari, Rima, Bhuvnesh Guglani, Nitij Gupta, and Sujata Chaturvedi. 2009. Intracranial epidermoid cyst: Magnetic resonance imaging features. *Neurology India* 57: 359–60. [CrossRef] [PubMed]

Law, Meng, Stanley Yang, Hao Wang, James S. Babb, Glyn Johnson, Soonmee Cha, Edmond A. Knopp, and David Zagzag. 2003. Glioma grading: Sensitivity, specificity, and predictive values of perfusion MR imaging and proton MR spectroscopic imaging compared with conventional MR imaging. *AJNR American Journal of Neuroradiology* 24: 1989–98. [PubMed]

Lee, Mark, Jeffrey H. Wisoff, Rick Abbott, Diana Freed, and Fred J. Epstein. 1994. Management of hydrocephalus in children with medulloblastoma: Prognostic factors for shunting. *Pediatric Neurosurgery* 20: 240–47. [CrossRef]

Levin, V., S. Liebel, P. Gutin, V. T. J. DeVita, S. Hellman, and S. A. Rosenberg. 2001. Neoplasms of the Central Nervous System (section 2). In *Cancer: Principles and Practice of Oncology*. Philadelphia: Lipincott, Williams, and Wilkins, pp. 2100–60.

Lindsay, K. W., I. Bone, and G. Fuller. 2011. *Neurology and Neurosurgery Illustrated. General Approach to History and Examination*. London: C L Elsevier.

Linos, Eleni, Tim Raine, Alvaro Alonso, and Dominique Michaud. 2007. Atopy and risk of brain tumors: A meta-analysis. *Journal of the National Cancer Institute* 99: 1544–50. [CrossRef]

Louis, David N., Arie Perry, Guido Reifenberger, Andreas Von Deimling, Dominique Figarella-Branger, Webster K. Cavenee, Hiroko Ohgaki, Otmar D. Wiestler, Paul Kleihues, and David W. Ellison. 2016. The 2016 World Health Organization Classification of Tumors of the Central Nervous System: A summary. *Acta Neuropathologica* 131: 803–20. [CrossRef]

Louis, David N., Arie Perry, Pieter Wesseling, Daniel J. Brat, Ian A. Cree, Dominique Figarella-Branger, Cynthia Hawkins, H. K. Ng, Stefan M. Pfister, Guido Reifenberger, and et al. 2021. The 2021 WHO Classification of Tumors of the Central Nervous System: A summary. *Neuro-Oncology* 23: 1231–51. [CrossRef]

Louis, David N., Hiroko Ohgaki, Otmar D. Wiestler, Webster K. Cavenee, Peter C. Burger, Anne Jouvet, Bernd W. Scheithauer, and Paul Kleihues. 2007. The 2007 WHO classification of tumours of the central nervous system. *Acta Neuropathologica* 114: 97–109. [CrossRef]

Love, J. Grafton, and And James W. Kernohan. 1936. Dermoid and epidermoid tumors (cholesteatomas) of central nervous system. *JAMA* 107: 1876–83. [CrossRef]

Luzzi, Sabino, Alice Giotta Lucifero, Jessica Rabski, Paulo A. S. Kadri, and Ossama Al-Mefty. 2023. The Party Wall: Redefining the Indications of Transcranial Approaches for Giant Pituitary Adenomas in Endoscopic Era. *Cancers* 15: 2235. [CrossRef] [PubMed]

Marchand-Crety, C., J. Riverain, Y. Drouet, F. Felici, C. L. Jeandidier, J. Thariat, and S. Servagi- Vernat. 2021. A new model outperforming RPA and DS-GPA scores for individualized survival prediction of patients following whole brain irradiation for brain metastasis. *Cancer/Radiothérapie* 25: 447–56. [CrossRef] [PubMed]

Marques, Pedro, and Márta Korbonits. 2017. Genetic aspects of pituitary adenoams. *Endocrinology and Metabolism Clinics of North America* 46: 335–74. [CrossRef]

Matula, C. 2012. Tuours of the pineal region. In *Principles of Neurosurgery*. Edited by Richard G. Ellenbogen and Laligam N. Shekhor. Philadelphia: Elsvier, pp. 565–78.

McEvoy, A. 2019. Dermoid and epidermoid cysts. In *Oxford Textbook of Neurological Surgery*. Edited by RRamez Kirollos, Adel Helmy, Simon Thomson and Peter Hutchinson. Oxford: Oxford University Press, pp. 197–203.

Mehdorn, H. Maximilian, Felix Schwartz, Stefan Dawirs, Jürgen Hedderich, Lutz Dörner, and Arya Nabavi. 2011. High-field iMRI in glioblastoma surgery: Improvement of resection radicality and survival for the patient? *Acta Neurochirurgica Supplement* 109: 103–6. [CrossRef] [PubMed]

Merchant, Thomas E., Chenghong Li, Xiaoping Xiong, Larry E. Kun, Frederic A. Boop, and Robert A. Sanford. 2009. Conformal radiotherapy after surgery for paediatric ependymoma: A prospective study. *The Lancet Oncology* 10: 258–66. [CrossRef] [PubMed]

Miller, Dorothea, Stefan Heinze, Wuttipong Tirakotai, Oliver Bozinov, Oguzkan Sürücü, Ludwig Benes, Helmut Bertalanffy, and Ulrich Sure. 2007. Is the image guidance of ultrasonography beneficial for neurosurgical routine? *Surgical Neurology* 67: 579–87. [CrossRef]

Morfouace, Marie, Anang Shelat, Megan Jacus, Burgess B. Freeman, David Turner, Sarah Robinson, Frederique Zindy, Yong-Dong Wang, David Finkelstein, Olivier Ayrault, and et al. 2014. Pemetrexed and gemcitabine as combination therapy for the treatment of Group 3 medulloblastoma. *Cancer Cell* 25: 516–29. [CrossRef]

Naik, Vismay Dinesh, and Nilay Rajendra Thakore. 2013. A case of symptomatic Rathke's cyst. *BMJ Case Reports* 2013: bcr2012006943. [CrossRef]

Nakau, H., T. Miyazawa, S. Tamai, K. Tsuchiya, K. Shima, T. Shirotani, and H. Chigasaki. 1997. Pathologic significance of meningeal enhancement ("flare sign") of meningiomas on MRI. *Surgical Neurology* 48: 584–90. [CrossRef]

Neil, Jayson A., and William T. Couldwell. 2019. Surgical management of sellar and suprasellar tumours. In *Oxford Textbook of Neurological Surgery*. Edited by Ramez Kirollos, Adel Helmy, Simon Thomson and Peter Hutchinson. Oxford: Oxford University Press, pp. 339–49.

Newton, Herbert B. 2016. Overview of brain tumor epidemiology. In *Handbook of Neurooncology Neuroimaging*. Edited by Herbert B. Newton. London: Elsevier.

Nimmannitya, Pree, Takeo Goto, Yuzo Terakawa, Hidetoshi Sato, Toshiyuki Kawashima, Hiroki Morisako, and Kenji Ohata. 2016. Characteristic of optic canal invasion in 31 consecutive cases with tuberculum sellae meningioma. *Neurosurgical Review* 39: 691–7. [CrossRef]

Norden, Andrew D., Patrick Y. Wen, and Santosh Kesari. 2005. Brain metastases. *Current Opinion in Neurology* 18: 654–61. [CrossRef] [PubMed]

Northcott, Paul A., Andrey Korshunov, Hendrik Witt, Thomas Hielscher, Charles G. Eberhart, Stephen Mack, Eric Bouffet, Steven C. Clifford, Cynthia E. Hawkins, Pim French, and et al. 2011. Medulloblastoma comprises four distinct molecular variants. *Journal of Clinical Oncology* 29: 1408–14. [CrossRef] [PubMed]

Oppenheim, H., and F. Krause. 1913. Operative erfolge bei geschwulsten derschuuugel und vierhugelgent. *Berliner Klinische Wochenschrift* 50: 2116–322.

Osborn, Anne G., and Michael T. Preece. 2006. Intracranial cysts: Radiologic-pathologic correlation and imaging approach. *Radiology* 239: 650–64. [CrossRef] [PubMed]

Ostrom, Quinn T., Haley Gittleman, Jordan Xu, Courtney Kromer, Yingli Wolinsky, Carol Kruchko, and Jill S. Barnholtz-Sloan. 2016. CBTRUS statistical report: Primary brain and other central nervous system tumors diagnosed in the United States in 2009–2013. *Neuro-Oncology* 18 S5: v1–v75. [CrossRef]

Ostrom, Quinn T., Haley Gittleman, Paul Farah, Annie Ondracek, Yanwen Chen, Yingli Wolinsky, Nancy E. Stroup, Carol Kruchko, and Jill S. Barnholtz-Sloan. 2013. CBTRUS statistical report: Primary brain and central nervous system tumours diagnosed in the United States in 2006–2010. *Neuro-Oncology* 15: ii1–ii56. [CrossRef]

Padma, M. V., S. Said, M. Jacobs, D. R. Hwang, K. Dunigan, M. Satter, B. Christian, J. Ruppert, T. Bernstein, G. Kraus, and et al. 2003. Prediction of pathology and survival by FDG PET in gliomas. *Journal of Neuro-Oncology* 64: 227–37. [CrossRef]

Pallud, Johan, Etienne Audureau, Marie Blonski, Nader Sanai, Luc Bauchet, Denys Fontaine, Emmanuel Mandonnet, Edouard Dezamis, Dimitri Psimaras, Jacques Guyotat, and et al. 2014. Epileptic seizures in diffuse low-grade gliomas in adults. *Brain* 137, Pt 2: 449–62. [CrossRef]

Pallud, Johan, Luc Taillandier, Laurent Capelle, Denys Fontaine, Matthieu Peyre, François Ducray, Hugues Duffau, and Emmanuel Mandonnet. 2012. Quantitative morphological magnetic resonance imaging follow-up of lowgrade glioma: A plea for systematic measurement of growth rates. *Neurosurgery* 71: 729–39. [CrossRef]

Pallud, J., P. Varlet, B. Devaux, S. Geha, M. Badoual, C. Deroulers, P. Page, E. Dezamis, C. Daumas-Duport, and F. X. Roux. 2010. Diffuse low-grade oligodendrogliomas extend beyond MRI-defined abnormalities. *Neurology* 74: 1724–31. [CrossRef]

Patel, Akash J., Dima Suki, Mustafa Aziz Hatiboglu, Hiba Abouassi, Weiming Shi, David M. Wildrick, Frederick F. Lang, and Raymond Sawaya. 2009. Factors influencing the risk of local recurrence after resection of a single brain metasrasis. *Journal of Neurosurgery* 113: 181–89. [CrossRef] [PubMed]

Poretti, Andrea, Avner Meoded, and Thierry A. G. M. Huisman. 2012. Neuroimaging of pediatric posterior fossa tumors including review of the literature. *Journal of Magnetic Resonance Imaging* 35: 32–47. [CrossRef] [PubMed]

Prabhu, Vikram C., and Henry G. Brown. 2005. The pathogenesis of craniopharyngiomas. *Child's Nervous System* 21: 622–27. [CrossRef] [PubMed]

Price, S. J., H. Bulstrode, and R. Mair. 2019. High-grade gliomas and molecular biology of neurosurgical oncology. In *Oxford Textbook of Neurological Surgery*. Edited by Ramez Kirollos, Adel Helmy, Simon Thomson and Peter Hutchinson. Oxford: Oxford University Press, pp. 89–106.

Price, Stephen J., R. Jena, N. G. Burnet, P. J. Hutchinson, A. F. Dean, A. Pena, J. D. Pickard, T. A. Carpenter, and J. H. Gillard. 2006. Improved delineation of glioma margins and regions of infiltration with the use of diffusion tensor imaging: An image-guided biopsy study. *AJNR American Journal of Neuroradiology* 27: 1969–74. [PubMed]

Raiyawa, Tassapong, Chonlakiet Khorprasert, Chawalit Lertbutsayanukul, Panya Seksarn, Darintr Sosothikul, Jiraphorn Amornfa, and Kanjana Shotelersuk. 2012. Management of intracranial germ cell tumours at the king Chulalongkorn Memorial Hospital. *Journal of the Medical Association of Thailand* 95: 1327–34.

Raza, Shaan M., Matei A. Banu, Angela Donaldson, Kunal S. Patel, Vijay K. Anand, and Theodore H. Schwartz. 2016. Sensitivity and specificity of intrathecal fluorescein and white light excitation for detecting intraoperative cerebrospinal fluid leak in endoscopic skull base surgery: A prospective study. *Journal of Neurosurgery* 124: 621–26. [CrossRef]

Rhoton, A. L., Jr. 2002. The Sellar Region. *Neurosurgery* 51: S335–S374. [CrossRef]

Rincon-Torroella, J., H. Brem, and Alfredo Quiñones-Hinojosa. 2017. Malignant Gliomas. Anaplastic Astrocytoma, Glioblastoma, Gliosarcoma, and Anaplastic Oligodendroglioma. In *Youmans & Winn Neurological Surgery*. Edited by H. R. Winn. Philadelphia: Elsevier, pp. 1006–25.

Ron, Elaine. 2003. Cancer risks from medical radiation. *Health Physics* 85: 47–59. [CrossRef]

Sakaki, Saburo, Sadanori Takeda, Hitoshi Fujita, and Shinsuke Ohta. 1987. An extended middle fossa approach combined with a suboccipital craniectomy to the base of the skull in the posterior fossa. *Surgical Neurology* 28: 245–52. [CrossRef]

Samii, M., and M. Tatagiba. 1992. Experience with 36 surgical cases of petroclival menigiomas. *Acta Neurochirurgica* 118: 27–32. [CrossRef]

Schweizer, Leonille, Christian Koelsche, Felix Sahm, Rosario M. Piro, David Capper, David E. Reuss, Stefan Pusch, Antje Habel, Jochen Meyer, Tanja Göck, and et al. 2013. Meningeal hemangiopericytoma and solitary fibrous tumors carry the NAB2- STAT6 fusion and can be diagnosed by nuclear expression of STAT6 protein. *Acta Neuropathologica* 125: 651–58. [CrossRef] [PubMed]

Senthilvel, Hari Nivas Periyakottai, Shyam Sundar Krishnan, and Madabhushi Chakravarthy Vasudevan. 2014. Extracranial infrasellar craniopharyngioma. *Neurology India* 62: 100–3. [CrossRef] [PubMed]

Sherman, Jonathan H., Kathryn Hoes, Joshua Marcus, Ricardo J. Komotar, Cameron W. Brennan, and Philip H. Gutin. 2011. Neurosurgery for brain tumors: Update on recent technical advances. *Current Neurology and Neuroscience Reports* 11: 313–19. [CrossRef] [PubMed]

Sibtain, N. A., S. Butt, and S. E. Connor. 2007. Imaging features of central nervous system haemangiopericytomas. *European Radiology* 17: 1685–93. [CrossRef]

Simpson, Donald. 1957. The recurrence of intracranial meningiomas after surgical treatment. *Journal of Neurology Neurosurgery and Psychiatry* 20: 22–39. [CrossRef]

Steno, Juraj, Martin Malacek, and Ivan Bizik. 2004. Tumor-third ventricular relationships in supradiaphragmatic craniopharyngiomas: Correlation of morphological, magnetic resonance imaging, and operative findings. *Neurosurgery* 54: 1051–58. [CrossRef]

Stummer, Walter, Uwe Pichlmeier, Thomas Meinel, Otmar Dieter Wiestler, Friedhelm Zanella, and Hans-Jürgen Reulen. 2006. Fluorescence-guided surgery with 5-aminolevulinic acid for resection of malignant glioma: A randomised controlled multicentre phase III trial. *The Lancet Oncology* 7: 392–401. [CrossRef]

Stupp, Roger, Warren P. Mason, Martin J. Van Den Bent, Michael Weller, Barbara Fisher, Martin J. B. Taphoorn, Karl Belanger, Alba A. Brandes, Christine Marosi, Ulrich Bogdahn, and et al. 2005. Radiotherapy plus concomitant and adjuvant temozolomide for glioblastoma. *The New England Journal of Medicine* 352: 987–96. [CrossRef]

Syro, Luis V., Leon D. Ortiz, Bernd W. Scheithauer, Ricardo Lloyd, Queenie Lau, Ricardo Gonzalez, Humberto Uribe, Michael Cusimano, Kalman Kovacs, and Eva Horvath. 2011. Treatment of pituitary neoplasm with temozolamide: A review. *Cancer* 117: 454–62. [CrossRef]

Taillibert, Sophie, and Jean-Yves Delattre. 2005. Palliative care in patients with brain metastases. *Current Opinion in Oncology* 17: 588–92. [CrossRef]

Takakura, Kintomo, K. Sano, S. Hojo, and A. Hirano. 1982. *Metastatic Tumors of the Central Nervous System*. New York: Igaku-Shoin.

Taylor, Michael D., Helen Poppleton, Christine Fuller, Xiaoping Su, Yongxing Liu, Patricia Jensen, Susan Magdaleno, James Dalton, Christopher Calabrese, Julian Board, and et al. 2006. Radial glia cells are candidate stem cells of ependymoma. *Cancer Cell* 9: P70. [CrossRef]

Thompson, Eric M., Thomas Hielscher, Eric Bouffet, Marc Remke, Betty Luu, Sridharan Gururangan, Roger E. McLendon, Darell D. Bigner, Eric S. Lipp, Sebastien Perreault, and et al. 2016. Prognostic value of medulloblastoma extent of resection after accounting for molecular subgroup: A retrospective integrated clinical and molecular analysis. *The Lancet Oncology* 17: 484–95. [CrossRef] [PubMed]

Tucha, Oliver, Christian Smely, Michael Preier, and Klaus W. Lange. 2000. Cognitive deficits before treatment among patients with brain tumors. *Neurosurgery* 47: 324–33. [CrossRef] [PubMed]

van den Bent, Martin J., Michael Weller, Patrick Y. Wen, Johan M. Kros, Ken Aldape, and Susan Chang. 2017. A clinical perspective on the 2016 WHO brain tumor classification and routine molecular diagnostics. *Neuro-Oncology* 19: 614–24. [CrossRef]

Van Effenterre, Rémy, and Anne-Laure Boch. 2002. Craniopharyngima in adult and children: A study of 122 surgical cases. *Journal of Neurosurgery* 97: 3–12. [CrossRef]

Vandeva, S., V. Vasilev, L. Vroonen, L. Naves, M-L. Jaffrain-Rea, A. F. Daly, S. Zacharieva, and A. Beckers. 2010. Familial pituitary adenomas. *Annales Endocrinologie* 71: 479–85. [CrossRef]

Van Wagenen, William P. 1931. A surgical approach for the removal of certain pineal tumours. *Surgery, Gynecology & Obstetrics* 37: 216–20.

Vellimana, A. K., G. P. Dunn, and I. F. Dunn. 2017. Intracranial Ependymomas in Adults. In *Youmans & Winn Neurological Surgery*. Edited by H. R. Winn. Philadelphia: Elsevier, pp. 1069–74.

WHO Classification of Tumours Editorial Board. 2021. *World Health Organization Classification of Tumours of the Central Nervous System*, 5th ed. Lyon: International Agency for Research on Cancer.

Willems, P. W., J. W. van der Sprenkel, C. A. Tulleken, M. A. Viergever, and M. J. Taphoorn. 2006. Neuronavigation and surgery of intracerebral tumours. *Journal of Neurology* 253: 1123–36. [CrossRef]

Yamamoto, Masaaki, Toru Serizawa, Takashi Shuto, Atsuya Akabane, Yoshinori Higuchi, Jun Kawagishi, Kazuhiro Yamanaka, Yasunori Sato, Hidefumi Jokura, Shoji Yomo, and et al. 2014. Stereotactic radiosurgery for patients with multiple brain metastases (JLGK0901): A multi-institutional prospective observational study. *The Lancet Oncology* 15: 387–95. [CrossRef]

Yuh, E. L., A. J. Barkovich, and N. Gupta. 2009. Imaging of ependymomas: MRI and CT. *Child's Nervous System* 25: 1203–13. [CrossRef]

Zigouris, Andreas, Dimitrios Pahatouridis, Evaggelos Mihos, George A. Alexiou, John Nesseris, Anastasia K. Zikou, Maria I. Argyropoulou, Anna Goussia, and Spyridon Voulgaris. 2009. Solitary cystic cerebral metastasis from transitional cell carcinoma of the bladder. *Acta Neurologica Belgica* 109: 322–25. [PubMed]